Development and Mechanical Characterization of Aluminum Hybrid Nanocomposite Reinforced with Alumina and Graphene Oxide

BY

TAWFEEQ ALAHMARI

A Thesis Presented to the
DEANSHIP OF GRADUATE STUDIES

KING FAHD UNIVERSITY OF PETROLEUM & MINERALS

DHAHRAN, SAUDI ARABIA

In Partial Fulfillment of the
Requirements for the Degree of

MASTER OF SCIENCE

In

MECHANICAL ENGINEERING

APRIL 2020

KING FAHD UNIVERSITY OF PETROLEUM & MINERALS

DHAHRAN- 31261, SAUDI ARABIA

DEANSHIP OF GRADUATE STUDIES

This thesis, written by **Tawfeeq Saad Alahmari** under the direction of his thesis advisor and approved by his thesis committee, has been presented and accepted by the Dean of Graduate Studies, in partial fulfillment of the requirements for the degree of **MASTER OF SCIENCE IN MECHANICAL ENGINEERING.**

THESIS COMMITTEE

Dr. Mohammed Abdul Samad
(Advisor)

Dr. Ihsan Ul-Haq Toor
(Member)

Morsi M. Mahmoud
Digitally signed by Morsi M. Mahmoud
DN: cn=Morsi M. Mahmoud, oid.EUPM, ou=ME, email=morsimahmoud@kfupm.edu.sa, c=SA
Date: 2020.06.24 23:05:28 +03'00'

Dr. Morsi Mohamed Mahmoud
(Member)

Zuhair Gasem
Digitally signed by Zuhair Gasem
DN: cn=Zuhair Gasem, o=KFUPM, ou=Chair, ME Dept., email=zuhair@kfupm.edu.sa, c=SA
Date: 2020.07.22 16:04:52 +03'00'

Dr. Zuhair Ghasem
Department Chairman

DEANSHIP OF GRADUATE STUDIES

Dr. Suliman Saleh Al-Homidan
Dean of Graduate Studies

Date

Dedication

Dedicated

To my beloved wife, brothers, sisters and well-wishers.

ACKNOWLEDGMENTS

All Praise and thanks to my God, for giving me the patience and health to complete this work. I acknowledge Sabic Company for giving me this opportunity and the required time to accomplish my thesis.

My sincere gratitude to My advisor Dr Mohammed Abdul Samad and committee members Dr. Ihsan Ul-Haq Toor and Dr. Morsi Mohamed Mahmoud who guided me with their dedicated attention, expertise and knowledge throughout my research. I'm grateful to Dr. Abbas Hakeem for his constructive guidance and support from CENT. Special thanks to Dr. Tahar Laoui for his support during the development phase to accomplish this project.

Special thanks to my colleagues in Mechanical Engineering Department and CENT for their help and support extended to me throughout this research.

My heartfelt gratitude to my beloved wife for her patience and continued prayers. My thanks also to all my family members for their encouragement.

Finally, I would like to extend my appreciation to King Fahd University of Petroleum and Minerals for accepting me on this program, providing me all the facilities and equipments to accomplish this research. I gratefully acknowledge the financial support provided by the Deanship of Scientific Research (DSR) at King Fahd University of Petroleum & Minerals (KFUPM) through Project No. IN151009.

TABLE OF CONTENTS

List of Figures

LIST OF TABLES

LIST OF ABBREVIATIONS/NOMENCLATURE

Al:	Aluminum
Al_2O_3:	Aluminum oxide
GO:	Graphene oxide
SPS:	Spark plasma sintering
CIP:	Cold isostatic press
HIP:	Hot isostatic press
BWR:	Ball to weight ratio
Vol.% :	Volume percent
T:	Temperature.
t :	time.
COF:	Coefficient of friction.
GNP:	Graphene nanoparticle.
SS:	Stainless steel.
PCA:	Process control agent.
Ar.	Argon gas.
GNS:	Graphene nano sheet.
P/M:	Powder metallurgy.
MMC:	Metal matrix composite.
MA:	Mechanical alloying
SEM:	Scanning electron microscope
XRD:	X-Ray diffraction
MPa:	Mega pascal

Wt.%:	Weight percent.
EDS:	Energy dispersive spectroscopy.
hr:	Hour
min:	Minutes
μm:	Micrometer
nm:	Nanometer
HV:	Vickers' hardness
PPM:	Parts per million.
CTE:	Coefficient thermal expansion
IUPAC:	International union of pure and applied chemistry.

Abstract

Name **Tawfeeq Saad Alahmari**

Title **Development and mechanical characterization of aluminum(Al) hybrid nanocomposite reinforced with alumina (Al_2O_3) and graphene oxide (GO).**

Department **Mechanical engineering**

Date **29/4/2020**

Aluminum matrix nanocomposites are one of the most frequently used metal matrix composites in several applications like aircraft, electronic industry, automobile, and aerospace due to their high strength to weight ratio, durability, structural rigidity and high corrosion resistance. However, owing to their low hardness and low wear resistance, their usage is limited in demanding applications especially in harsh environment. So, in this research, we developed an aluminum hybrid nanocomposite reinforced with alumina (Al_2O_3) and graphene oxide (GO), to obtain a hybrid nanocomposite with the best of the individual properties of both reinforcements. The focus of the study was to optimize the Al_2O_3 and GO contents in the composite that will impart a good mechanical and thermal properties such as high hardness, compressive strength, heat flow and thermal expansion. In this research, powder metallurgy technique and Spark Plasma Sintering were used to develop the hybrid nanocomposite samples. Differential scanning calorimetry (DSC) was used to examine the role of reinforcements on the thermal properties of the aluminum matrix. Characterization techniques such as FESEM, EDS, XRD and Raman spectroscopy were used to investigate the morphology of the developed samples. In the first phase, different volume percents of alumina (10%, 20%, 30%) were used as a reinforcement to prepare with (Al-X%Al_2O_3) nanocomposites to get the optimum volume percent of Al_2O_3 resulting in a good mechanical properties, which was found to be 10 vol% of Al_2O_3. In the second phase, a hybrid nanocomposite was developed by reinforcing the Al-10% Al_2O_3 with different weight percents (0.25%, 0.5%, 1%) of GO to obtain the optimum nanocomposite with improved mechanical/thermal properties. Results revealed that the (Al-10 vol%Al_2O_3 -0.25wt.%) GO hybrid nanocomposite showed the highest improvement of 13% in hardness and the highest improvement of 30% in compressive strength as compared to the (Al-10 vol% Al_2O_3) nanocomposite. Moreover, the hybrid nanocomposite (Al-10% Al_2O_3-0.25%) GO also showed the lowest thermal expansion.

MASTER OF SCIENCE DEGREE
KING FAHD UNIVERSSITY OF PETROLEUM AND MINERALS, SAUDI ARABIA

ملخص الرسالة

الاسم/ توفيق سعد الأحمري

الموضوع/ تطوير وتشخيص ميكانيكي لمعدن الألمونيوم وذلك بتهجين ذرات اكسيد الالمونيوم متناهيه الصغر وأكسيد القرافين كمعززات لخصائص الألمونيوم.

القسم/ الهندسة الميكانيكية.

التاريخ:1441/9/6

مركبات مصفوفة الألمنيوم هي واحدة من مركبات مصفوفة المعادن الأكثر استخدامًا في العديد من التطبيقات مثل الطائرات، والصناعات الإلكترونية ، والسيارات ، والفضاء بسبب قوتها العالية إلى نسبة الوزن، والمتانة، والصلابة الهيكلية ومقاومة الاحتكاك العالية. ومع ذلك ، نظرًا لصلادتها المنخفضة ومقاومة التآكل المنخفضة ، فإن استخدامها محدود في التطبيقات الصعبة خاصة في البيئات القاسية. لذلك ، قمنا في هذا البحث بتطوير مركب نانو هجين من الألمنيوم مدعم بالألومينا وأكسيد الجرافين ، للحصول على مركب هجين مع أفضل الخصائص الفردية لكل من التعزيزات المستخدمة. ركزت الدراسة على تحسين نسب محتويات الألومينا وأكسيد الجرافين في مركب الألومنيوم باستخدام طريقة ضغط المسحوق (التلبيد) وتقنية سبارك بلازما والذي ستضفي خصائص ميكانيكية وحرارية جيده مثل الصلابة العالية، قوة الضغط، التدفق الحراري والتمدد الحراري. ايضا تم استخدام اجهزه مخبريه ذات تقنية عالية لدراسة مورفولوجيا العينات المطورة كالماسح الضوئي التفاضلي والمتقدم، اشعة اكس، جهاز الطيف الضوئي ومجهر رامان. في المرحلة الأولى من المشروع كان التركيز على الحصول على افضل الخواص الميكانيكية والحرارية من خلال استخدام نسب مختلفة من الألومينا (10%، 20%،30 %) والتي كانت متوفرة في نسبة الألومينا ذات الحجم 10%. في المرحلة الثانية من المشروع، تم تطوير مركب الومنيوم نانوي هجين باستخدام نسبة الحجم المثالي من الألومينا المنتجة في المرحلة الاولى مع نسب مختلفة من اكسيد الجرافين(0.25%، 0.50%، 1%) للحصول على مركب نهائي ذات خصائص ميكانيكية وحرارية عالية فيما أظهرت النتائج ان مركب الألومنيوم الهجين ذا النسب (0.25% من اكسيد الجرافين و10% من الألومينا) اثبت نسبة تحسن بمقدار 13% في الصلابة ونسبة 30% في قوة الضغط مقارنه مع مركب الألومنيوم الذي يحتوي فقط على 10% من حجم الألومينا، كما اثبتت النتائج بأنه اقل نسبة تمدد حراري مقارنة مع المركبات المنتجة.

درجة الماجستير

جامعة الملك فهد للبترول والمعادن، المملكة العربية السعودية

CHAPTER 1

INTRODUCTION

Metal matrix composites (MMCs) are one of the most important developments in the field of engineering materials. Defined as a combination of two or more constituent materials so that the two materials work together to give the composite unique properties. It is made of a reinforcing phase, which might be in the form of fibers, sheets, or particles, embedded in other material called matrix, which is representing the greater quantity of the composite[1]. Typically, these materials have the ability to combine the properties of reinforcing phase with that of the matrix. Thus, composite materials have the capability to serve a wide spectrum of applications. Nanocomposite is defined as a composite material where at least one of its constituent dimensions is in the nanometer size scale (< 100 nm) [2]. The challenge in developing nanocomposites is to find ways to create macroscopic components that avail from the unique physical and mechanical properties of nanoparticles. Various processes that have been proposed to obtain nanocomposite materials follow two main approaches: Top down and bottom up.

Top-down is characterized by the production of nano products departing from normal size materials i.e., reducing the dimensions of the original material by using special size reduction techniques. Bottom-up approach is related to the "synthesis" of nano sized materials starting from the molecular scale as shown in Figure 1.1 for example, the formation of particles by precipitation from a fluid phase [2].

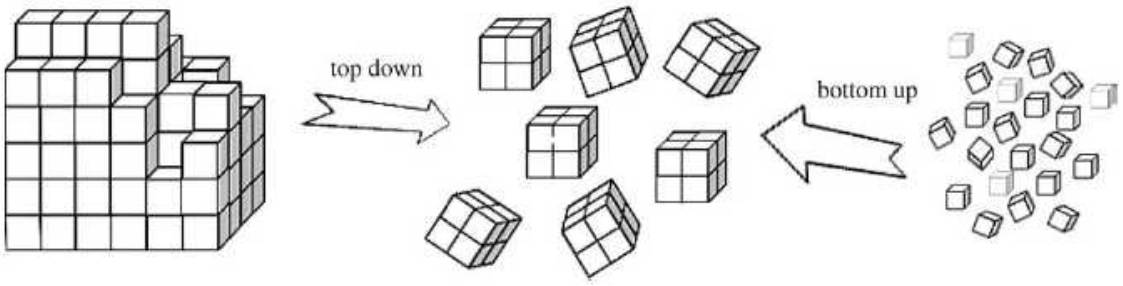

Figure 1.1 : Top-down and bottom-up approaches

1.1 Classification of composite/nanocomposite materials

Composites are classified into three categories depending on their matrix:

i. **Metal matrix composites (MMC):** is a group of material such as (metals, alloys or intermetallic compound) incorporated with various reinforcing phases such as whiskers, particulates or continuous fibers.

ii. **Polymer matrix composites (PMC):** is a material consisting of polymer (resin) matrix combined with a fibrous reinforcing dispersed phase. Polymer matrix composite can be classified into thermoplastic polymer which is linear or branched polymers. In which, the chains of molecules are not interconnected to each other. Thermosetting polymers are heavily cross linked to produce a strong three dimensional network structure.

iii. **Ceramic matrix composites (CMC):** is a subgroup of composite material that consists of ceramic fibers embedded in a ceramic matrix

1.2. Hybrid composites/nanocomposites

Hybrid composites are a new class of material consisting of two or more different type, size and shape of reinforcements that offer better mechanical/thermal properties than a single reinforcement. Hybrid composites help to improve the mechanical properties of the composites by

taking the advantages of the individual properties of the combined reinforcements. Therefore, it has become a point of attraction for many applications [36].

1.3. Aluminum composites

The current engineering applications requires material that are stronger, lighter and less expensive [35]. Aluminum (Al) is an excellent choice for these demanding applications due to its high strength to weight ratio and high corrosion resistance. However, its usage in the engineering applications is limited due to its inferior mechanical properties, such as moderate strength and elastic modulus and low wear resistance. Hence, reinforcing aluminum with a strong, stiff and a light weight phase or phases will help to increase its mechanical and thermal properties[6].

1.4. Alumina (Al_2O_3) as a reinforcement

Ceramic particles such as alumina (Al_2O_3) are an excellent choice as a reinforcement to improve the properties of aluminum [6]. Aluminum oxide is a favorable filler in metal composites [35]. It does not react with the metal matrix at high temperatures and does not create undesired phases[35]. On top of that, it also helps in increasing the hardness and improving the tribological properties of the metal matrix. Alumina is one of the most cost effective and widely used material in the family of engineering ceramics materials. It possesses strong ionic interatomic bonding, giving rise to its desirable material characteristics. It can exist in several crystalline phases which all revert to the most stable hexagonal alpha phase at elevated temperatures. Alumina has several features enable the researchers to use it in many applications to improve hardness, wear resistance, thermal conductivity, strength and stiffness of different metals[33]. Alumina particles were used to enhance the mechanical properties of aluminum [21].

They found that the hardness of aluminum increased with increasing alumina content as shown in Figure (1.2). The authors attributed this improvement to the amount of hard alumina (Al_2O_3) particles in the soft aluminum matrix and formation of good interface between aluminum matrix and alumina Al_2O_3.

Wear tests were carried out to evaluate the contribution of alumina particles in the aluminum matrix at different loads. Researcher found that, the wear rate is decreasing with increasing the amount of alumina content, sliding distance due to higher load-bearing capacity of hard reinforcing material and good interfacial bonds between the alumina particles and aluminum matrix[21].

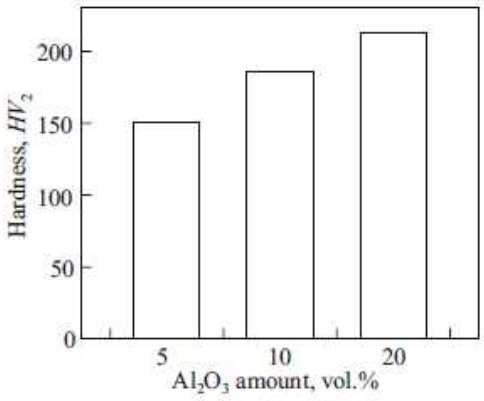

Figure 1.2 Effect of Al_2O_3 content on the hardness of Al–Al_2O_3 composites

1.5 Graphene oxide (GO) as a reinforcement

In simple terms, Graphene, is a thin layer of pure carbon; it is a single, tightly packed layer of carbon atoms that are bonded together in a hexagonal honeycomb lattice. In more complex terms, it is an allotrope of carbon in the structure of a plane of sp_2 bonded atoms with a molecule bond length of 0.142 nanometres[4,5]. The term ‘‘Graphene’’ was recommended by the relevant

IUPAC commission to replace the older term ‘‘graphite layers’’ that was unsuitable in the research of single carbon layer structure, because a three-dimensionally (3D) stacking structure is identified as ‘‘graphite’’. The recent definition of graphene can be given as a two-dimensional monolayer of carbon atoms, which is the basic building block of graphitic materials. Graphene of two-dimensional material, offers unique friction and wear properties that is not typically seen in conventional materials[6]. Graphene can serve as a solid or colloidal liquid lubricant. The term Graphene is typically applied to a single layer of graphite, although common references also exist to bilayer or trilayer Graphene[7]. Graphene has been used in several researches as a reinforcement in aluminum matrix. One of these studies, it has been found that the Graphene nano particles increased the tensile strength and yield strength of aluminum matrix gradually with an addition up to 1wt% by 84.5% and 54.8%, respectively, because of the good dispersion and strong interfacial bonding between aluminum and graphene nano particles[34]. On the other hand, increasing the graphene nano particles, will reduce the composite ductility. Researchers attributed this effect to the pinning effect of graphene on the boundaries of matrix, whereby, graphene can restrict the grains from deformation by hindering the dislocation movement.

1.6 Spark plasma sintering (SPS)

Spark plasma sintering also referred to electric field assisted sintering (EFAS), field assisted sintering technique (FAST), plasma assisted sintering (PAS) and plasma pressure consolidation (PPC) is a newly developed sintering process that combines the use of mechanical pressure and microscopic electric discharge between the particles. The enhanced densification in this process has been attributed to a localized self-heat generation by the discharge, activation of the particle surfaces, and high speed of mass and heat transfer during the sintering process. As a result, samples can rapidly reach full density at relatively low temperature. The equipment consists of a

mechanical device capable of applying uniaxial pressure and electrical components to apply the pulsed and steady DC current. The loose powders are directly loaded into a punch and die unit without any additives. Graphite die and punches are commonly used. This limits the pressure levels to low values, generally<100MPa. Although, high pressure graphite may also be available. The pressure may be constant throughout the sintering cycle or changed in different densification stages. The graphite confinement provides a reducing component to the sintering environment. The machines are equipped with chambers for vacuum and controlled environment. A typical pulse discharge is achieved by the application of low voltage (~30V) and ~1000A current. The duration of each pulse may be varied between 1 to 300ms, on/off pulses may have different durations. The pulses are applied throughout the whole sintering cycle in SPS. The pulsed current promotes electrical discharges at powder particle surfaces. Thus, activating them for subsequent bonding. The main benefit of enhance sintering is a short densification time usually associated with minimal grain growth [17].Schematic of SPS is illustrated in Fig.(1.3).

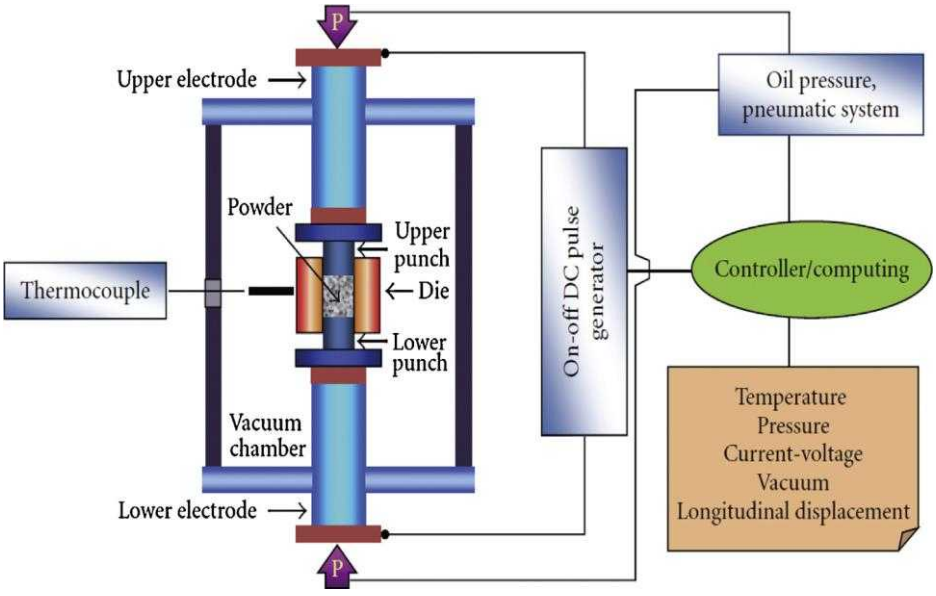

Figure 1.3. Schematic of spark plasma sintering[6]

1.7 Defining the problem statement

Aluminum hybrid nanocomposite is playing an important role in various academic and industrial fields such as aerospace, automobile and electronic industry. However, owing to their low hardness and low wear resistance, their usage is limited in demanding applications especially in harsh environments. So, in order to bridge this gap, we proposed to develop an aluminum hybrid nanocomposite reinforced with alumina and graphene oxide. These two fillers are promising materials to help in improving the mechanical and thermal properties of aluminum matrix. Hence, based upon this survey, we defined the main objective of our current study as follows:

1.8 Objective

To develop aluminum hybrid nanocomposite reinforced with alumina and graphene oxide using ball milling and Spark Plasma Sintering techniques for improved mechanical and thermal properties.

To achieve the above objective, the project was divided into three phases which are as follows:

1.9 Project phases

Phase 1: The focus of this phase is to develop and characterize the aluminum nanocomposite reinforced with different volume % of alumina (Al_2O_3) using the ball milling and SPS techniques to obtain the optimum volume % of Al_2O_3 resulting in the best mechanical properties.

- Task 1: Characterize the as received materials (Al, Al_2O_3, GO) by SEM and XRD
- Task 2: Ball milling of aluminum and different volume % of alumina to obtain a well dispersed mixture.

- Task 3: Conduct spark plasma sintering for the mixed (Al- X % Al_2O_3 powders to obtain solid samples)
- Task 4: Conduct hardness and density tests.
- Task 5: Characterize the prepared samples using FESEM to investigate the morphology.

Phase 2: The focus of this phase is to develop and characterize the aluminum hybrid nanocomposites reinforced with the optimum volume percent of alumina found from Phase 1 and with different weight % of graphene oxide using the ball milling and spark plasma sintering techniques.

- Task 1: Mixing different wt.% of GO with the optimum volume % of Al_2O_3 in the aluminum matrix by using ball milling.
- Task 2: Conduct spark plasma sintering to prepare samples from the mixture prepared.
- Task 3: Conduct density and hardness tests.
- Task 4: Characterize the samples using FESEM to investigate the morphology.

Phase 3: The focus of this phase is to characterize the optimum hybrid aluminum composite resulting from Phase 2 by using different mechanical and thermal tests.

- Task 1: Conduct the differential scanning calorimetry (DSC)
- Task 2: Conduct compression test.
- Task 3: Conduct thermal expansion test

1.10 Research methodology

The research work intended to be undertaken in three phases, each phase has a clear milestone presented in the below chart Fig (1.4)

Phase 1

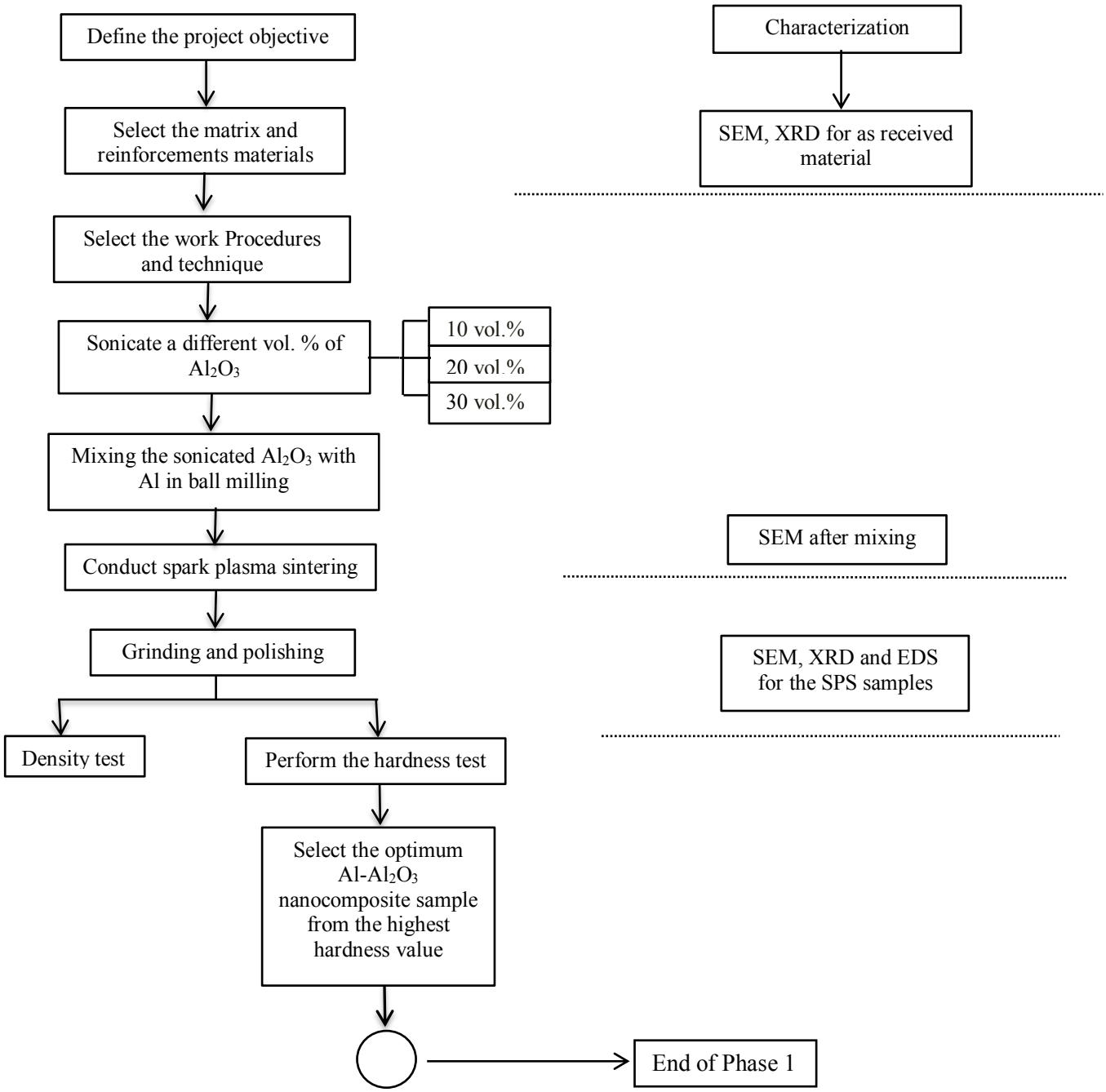
Define the project objective
Select the matrix and reinforcements materials
Select the work Procedures and technique
Sonicate a different vol. % of Al_2O_3
10 vol.%
20 vol.%
30 vol.%
Mixing the sonicated Al_2O_3 with Al in ball milling
Conduct spark plasma sintering
Grinding and polishing
Density test
Perform the hardness test
Select the optimum Al-Al_2O_3 nanocomposite sample from the highest hardness value
End of Phase 1
Characterization
SEM, XRD for as received material
SEM after mixing
SEM, XRD and EDS for the SPS samples

Phase 2

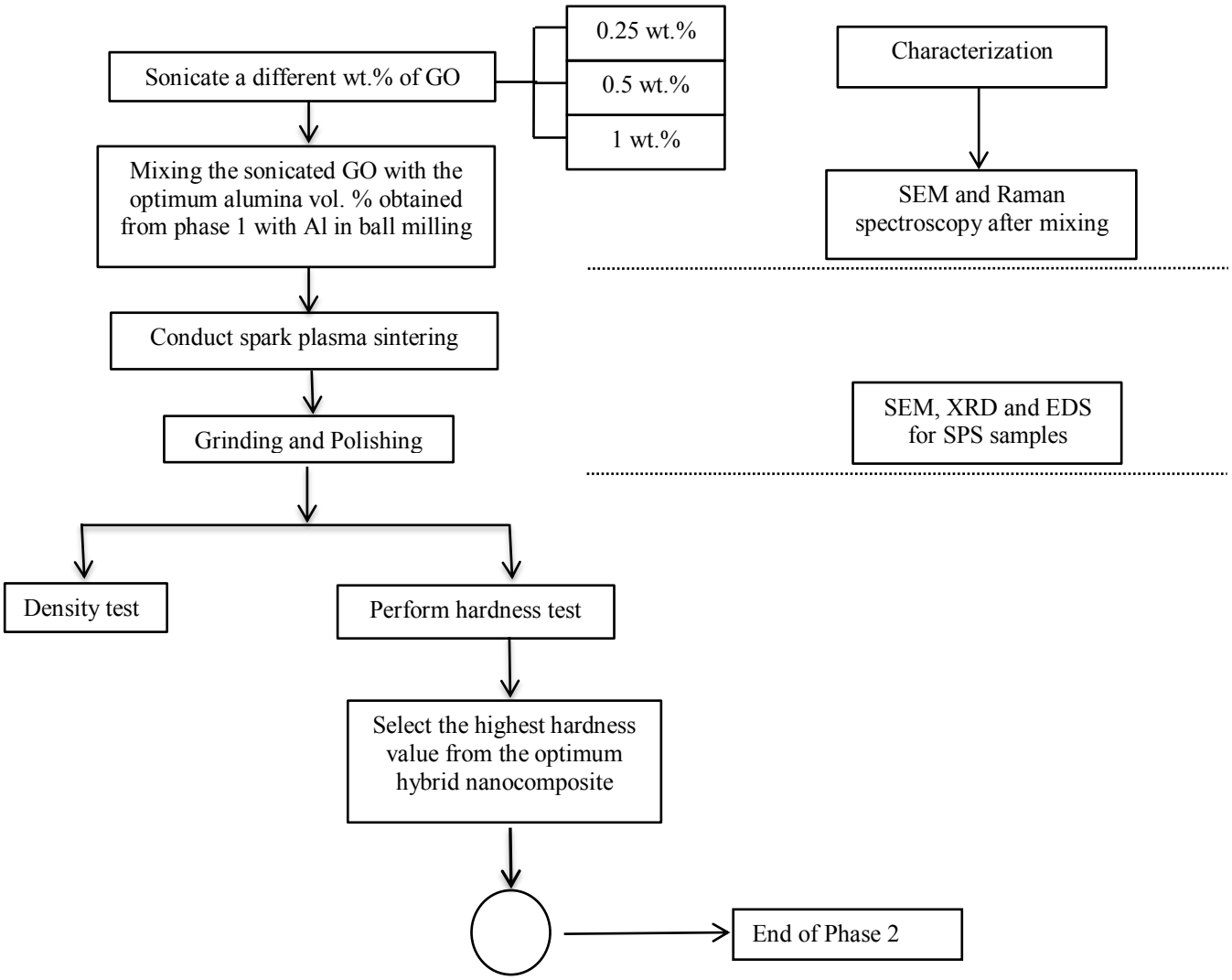
Sonicate a different wt.% of GO
0.25 wt.%
0.5 wt.%
1 wt.%
Mixing the sonicated GO with the optimum alumina vol. % obtained from phase 1 with Al in ball milling
Conduct spark plasma sintering
Grinding and Polishing
Density test
Perform hardness test
Select the highest hardness value from the optimum hybrid nanocomposite
End of Phase 2
Characterization
SEM and Raman spectroscopy after mixing
SEM, XRD and EDS for SPS samples

Phase 3

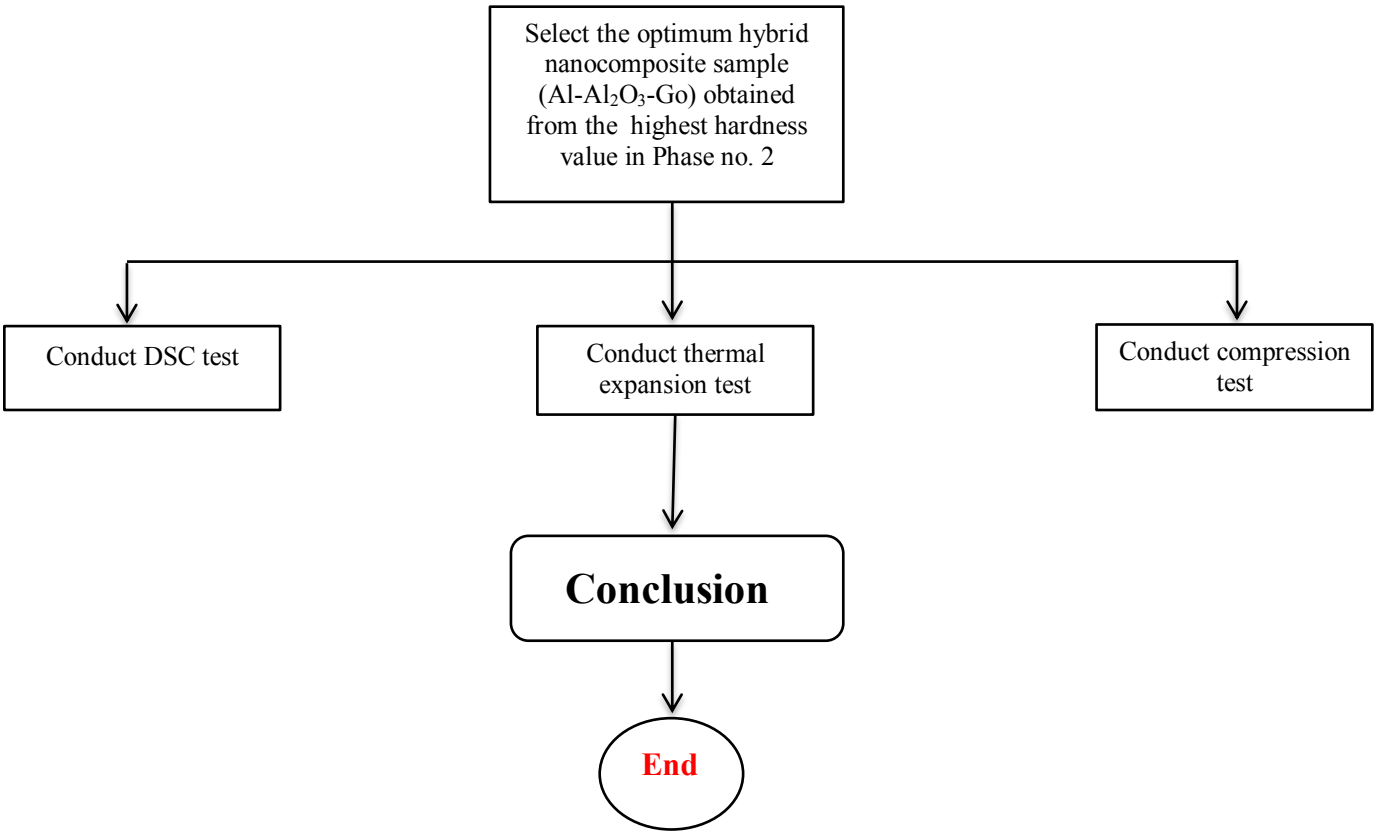

Figure1.4. Flow chart of research methodology.

CHAPTER 2

LITERATURE REVIEW

2.1 Processing techniques

Processing of metal matrix composite is classified into two main groups (in-situ and ex-situ synthesis). In ex-situ synthesis, the particles are added into a metal matrix from outside to inside. Whereas in, in-situ synthesis which is shown in Fig (2.1), the reinforcement is utilized by a chemical reaction or exothermic reaction [3]. It can be achieved through (i) gas-liquid (ii) liquid-liquid (iii) solid-liquid reactions[18]. The processing techniques are explained in detail as follows:

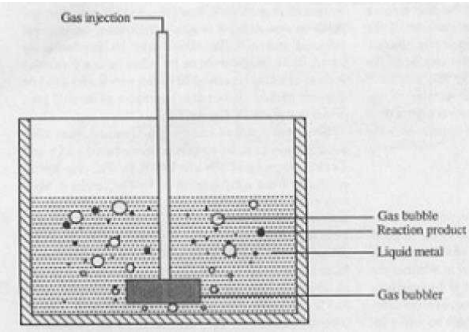

Figure 2.1 In situ process.

2.1.1. Liquid state: In this method, the continuous phase (matrix) which is in the liquid state and the discontinuous phase (reinforcement) are blended together. Liquid state involves: stir casting, squeeze casting and compo casting methods [3].

2.1.2. Solid state: Solid state involves: powder metallurgy (PM), immersion plating, spray deposition, diffusion bonding and electroplating[3].

2.1.3. Stir casting: In this process, the discontinuous reinforcement phases are blended into the matrix when it is in a molten form by a mechanical stirrer. Stir casting involves stirring the melt with a solid ceramic particles, then allowing the mixture to be solidified. This process can be done by using a conventional equipment on a continuous or semi- continuous basis. Stir casting usually involves a prolonged liquid-ceramic contact which can be a cause of substantial interfacial reaction[9]. Stir casting method is applied for mass production of metal matrix composites. The advantages of this method are low cost, simple processing route and uniform dispersion of nano particles. So, it is a recommended process in fabricating metal matrix nanocomposites[3]. Fabrication process of stir casting is illustrated in Fig.(2.2).

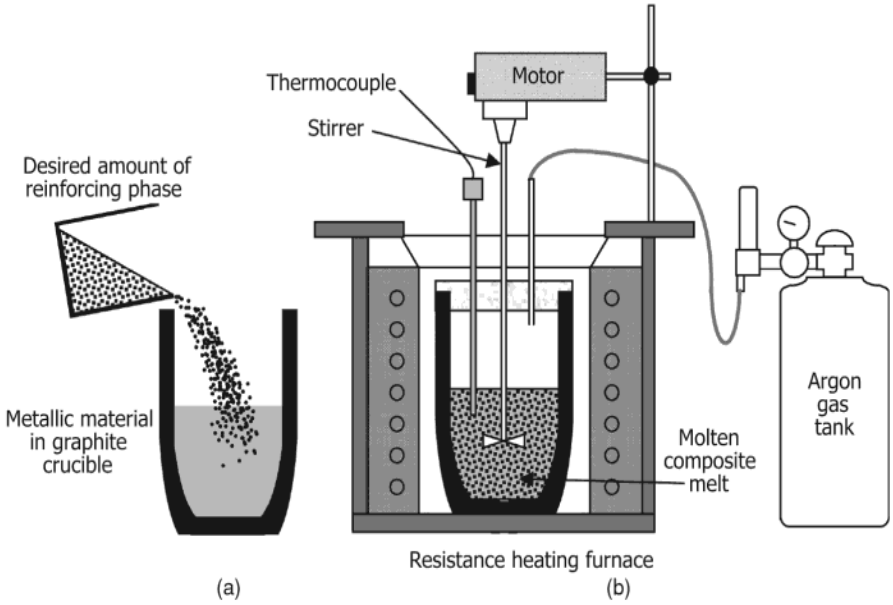

Figure 2.2 Schematic of stir casting process

2.1.4. Compo casting: Is a process when the reinforcement particles are added to the solidifying melt. The primary solid particles are formed in the semi-solid melt which can be a cause of entrapment of the reinforcement particles [2].

2.1.5. Squeeze casting: In this process, the molten metal with an adequate superheat is poured into a die with closed ends. It solidifies to get the desired shape. Consequently, this process is a combination of gravity die casting and closed die forging [10]. This method can be divided into two main processes(direct and indirect squeeze casting) as classified in Fig(2.3): The squeeze casting process is illustrated in Fig(2.4)

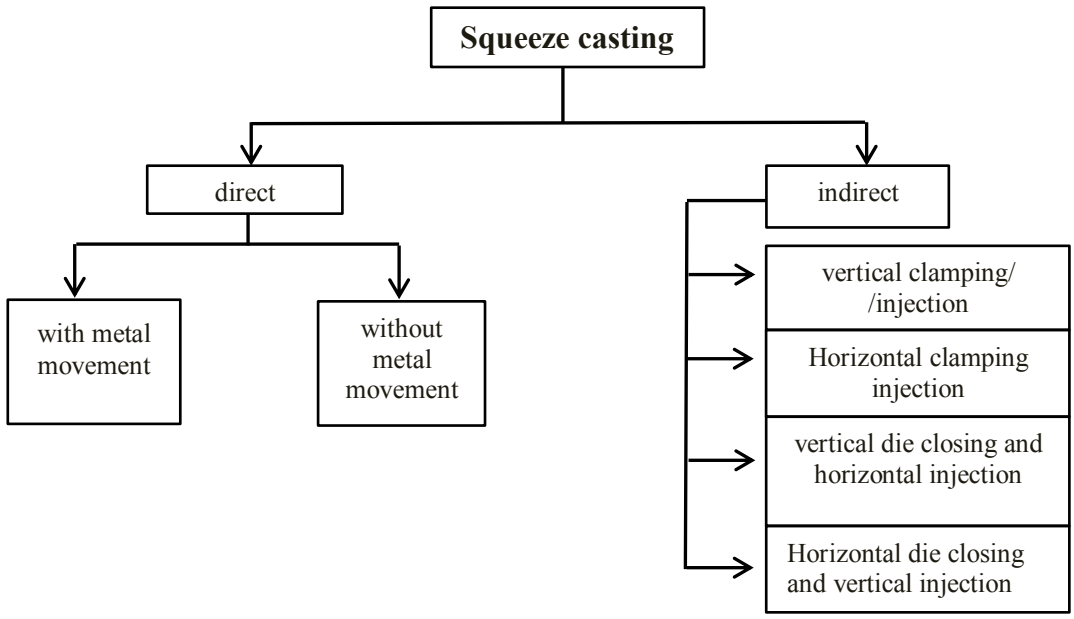

Figure 2.3 Types of squeeze casting

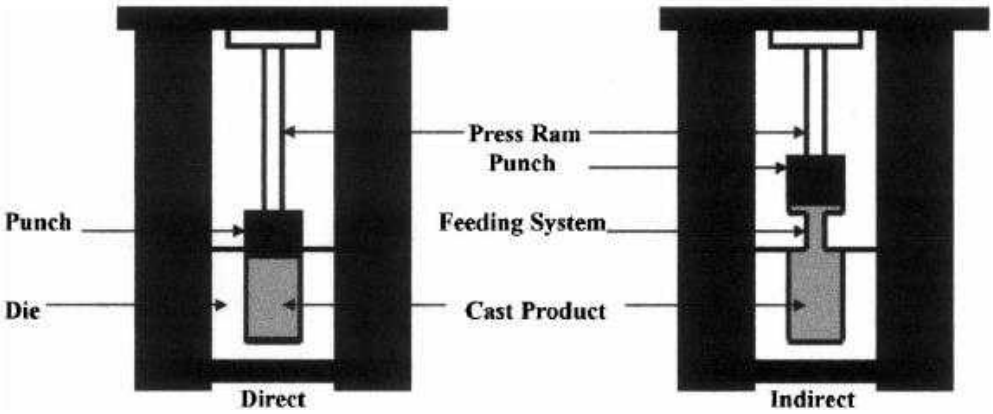

Figure 2.4 Squeeze casting processes

2.1.6. Spray casting/deposition methods: In this process, atomized of molten droplets with very high speed are impressed on a preheated substrate, the reinforcing particles are also impacted with the melt spray allowing the reinforcement particles to be engulfed in the molten material to form a composite[11].

2.1.7. Powder metallurgy(P/M): is one of the process methods used to produce aluminum matrix, which involves mixing the powder matrix with addition of reinforcements, followed by compaction and sintering [1]. One of the several advantages of P/M route over the other techniques is that of easily obtaining the composite due to the uniform distribution of reinforcements especially for (particles, whiskers). Moreover, particles are homogeneously distributed in the mixture to obtain a good microstructure. Powder metallurgy process steps are explained in Fig.(2.5).

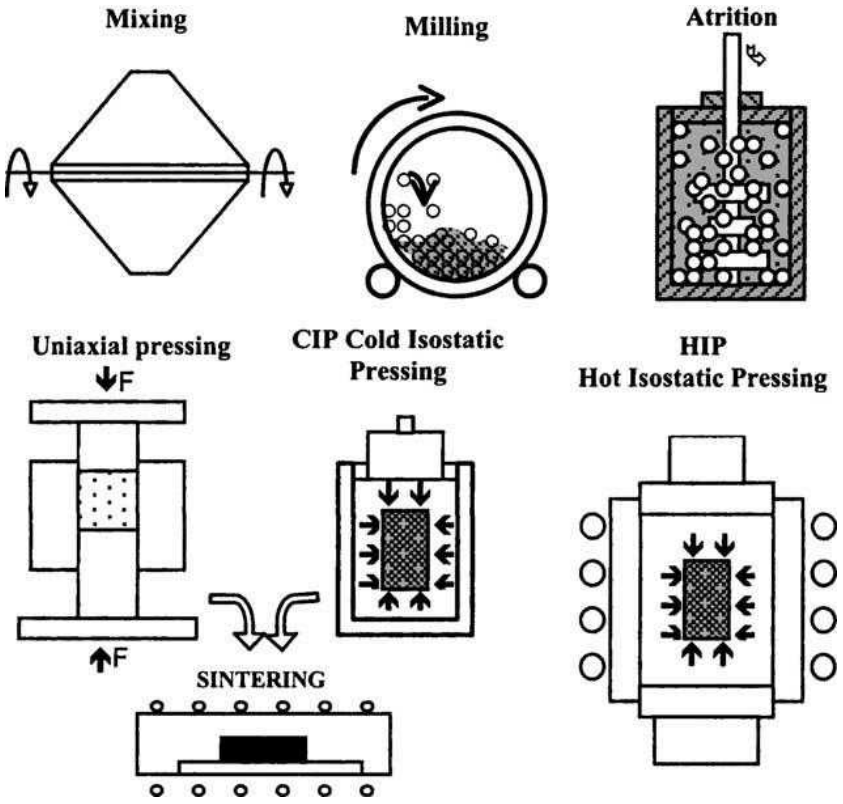

Figure 2.5 Powder metallurgy process steps

2.1.8. Mechanical alloying(MA): is a powder processing technique that helps in obtaining homogeneous materials from blended elemental mixtures. Mechanical alloying (MA) is a process in which a mixture of powders (metals or alloys/compounds) are milled together [12]. The process of (MA) consists of loading the powder and grinding medium (generally hardened steel or tungsten carbide balls) in a container sealed under a protective argon atmosphere (to avoid oxidation during milling) and milled based on the given process parameters. A few amount of process control agent (PCA) is normally added to prevent excessive cold welding amongst the powder particles [10]. Various types of mills generally are used such as shaker mills (wherein about 10 g of the powder can be processed at a time), Attritor mill (where a large quantity of powder can be processed at a time), or Fritsch Pulverisette mill (where a powder is in more than one container can be processed simultaneously) [10].

2.1.9. Ball milling: Is the process in which the balls are usually made of heavy material, fall and crush the powder intended to be milled. By repeating the same actions several times, the particles size of the powder is reduced to fine particles. [13]. Fig (2.6) shows the process steps of ball milling.

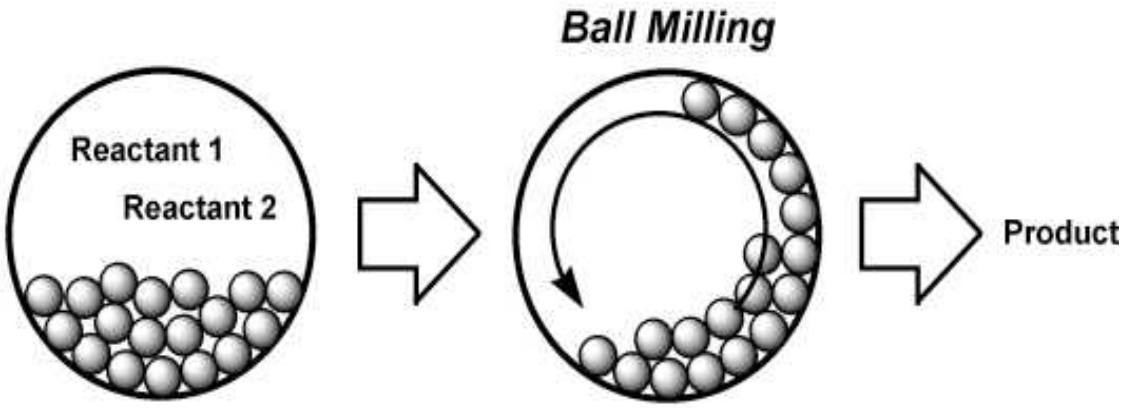

Figure 2.6 Ball milling process.

2.2 Types of mills

2.2.1 Shaker mills: Shaker mills such as SPEX mills which is presented in (Fig. 2.7), have about 10 to 20g of the powder at a time. It is the most commonly used mill for laboratory investigations and alloy screening purposes. The common type of the mill has one vial, containing the sample and the grinding balls, which is secured in a clamp and moves energetically back and forth several times a minute. The back and forth shaking motion is combined with a lateral movement of the vials [11].

Figure 2.7 SPEX 8000 mill.

2.2.2 Planetary ball mill: Is one of the most popular mills used for conducting mechanical alloying experiments, whereby a few hundred grams of powder can be milled at a time.

Planetary ball mill is arranged on a rotating support disk and special drive mechanism to rotate around their own axes. The centrifugal force which is produced by rotating the vials will crush the powders with the help of grinding balls[11]. Planetary ball mill, Pulverisette type, is showing in Fig(2.8)

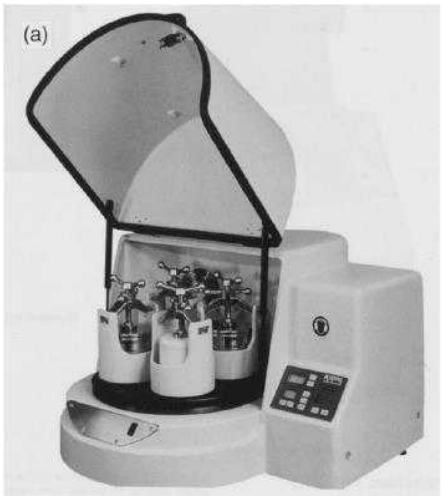

Figure 2.8 Pulverisette planetary ball milling equipment.

2.2.3 Attritor mill: Is consists of a rotating shaft with disc, stationary drum and grinding media as show in Fig.(2.9). Powder is placed in the drum with the grinding media. The rotating shaft will agitate the powder and the grinding media. As a result, the powder is homogenously dispersed. The rate of grinding is increases as the speed of rotating shaft increases [11].

Figure 2.9 Model HD-01/HDDM-01attritor mill, union process

2.3 Powder compaction

Is the process of compacting the metal powder in a die through the application of high pressures[14]. Several methods have been used to compact nanocrystalline powders into green bodies. The most commonly used pressing processes in the powders are:

1. Uniaxial Pressing. 2. Isostatic Pressing.

Uniaxial pressing: There is a cold compaction and hot compaction approaches. In both approaches, it is essential to use an inert gas atmosphere to prevent the oxidation due to the presence of very fine particles and the long compaction duration at elevated temperature. Fig(2.10) shows the process steps for this method.

Isostatic pressing: The pressure is applied from all directions. Thus, the term “isostatic” is used in either a gas or liquid. Uniform compaction pressure is achieved throughout the powder compact. The isostatic pressing is divided into two types:

i) Cold isostatic pressing (CIP)

ii) Hot isostatic pressing (HIP)

Cold isostatic pressing usually results in a uniform densification when compared to cold uniaxial compaction because of frictional force between the powder and the die in the uniaxial pressing. However, the isostatic pressing method, is only used to produce small quantities and for simple shaped materials due to its higher production cost and slower processing speed[14].

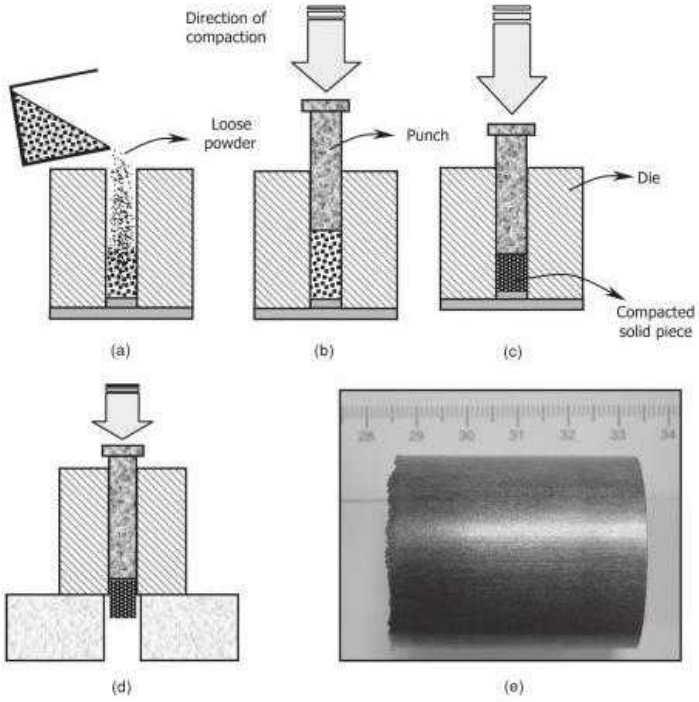

Figure 2.10 Schematic diagrams showing the uniaxial pressing powder steps (a) Filling the die cavity with loose powder particles (b), (c) Applying uniaxial pressure to compact the powder (d) Removing the compacted solid piece from the die (e) Compacted magnesium nanocomposite billet.

2.4 Sintering

Is the process of compacting and forming a solid mass of material by means of heat or pressure without melting the material until the powder particles coalesce. The atoms in the material

diffuses across the boundaries of the particles. Thereby, the particles fuse together creating one solid body[15].

2.4.1 Mechanism of sintering

When a powder compact is heated up to 70% to 90% of its melting temperature, sintering can occur. Sintering is usually divided into two overlapping stages. During the first stage, the particles are bonded together due to the necks growing between the particles. The density of the compacted particles increases during the second stage because of the elimination of pores. The driving force in both stages is the excessive surface free energy. Five mass transfer mechanisms are responsible for the growth of necks and for the pore shrinkage [15]. Further explanation for the sintering mechanism can be seen from Fig (2.11).

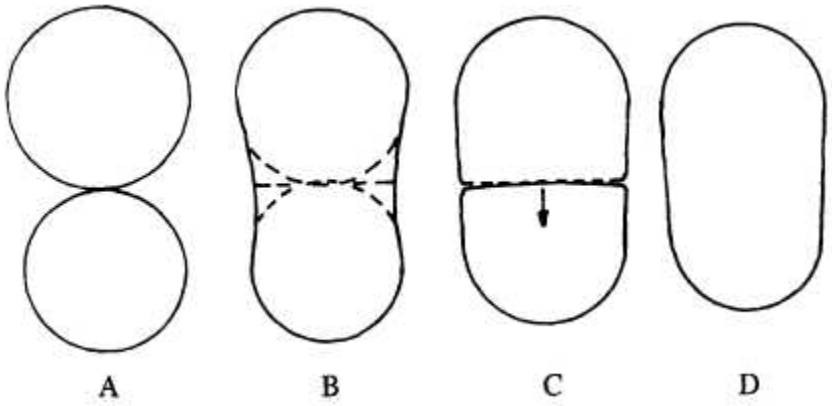

Figure 2.11. Sintering mechanism

Four stages for grain in very porous compacts.

A) Two particles come in contact with each other.

B) A neck grows between the two particles and the grain boundary appears at the contact interface.

C) The grain boundary migrates towards the center of curvature.

D) An elongated particle has been formed[15].

2.5 Synthesis of aluminum(Al) and alumina(Al_2O_3) composites

- M. Karbalaei Akbari et al used stir casting method to fabricate 1.5vol% of alumina with aluminum matrix to study the effect of milling time on the mechanical properties of the composites such as: hardness, tensile, and compression tests. In this review, the author reported that porosity level slightly increased with increasing the milling time. However, hardness, tensile, and compressive strength decreased with increasing the milling time due to gradual oxidation of metallic powders during the milling process. Increasing the milling time leads to a gradual reduction in the mechanical performance of the samples. The author reported that, the hardness values of the composites linearly decreased with an increase in the the milling time owing to the following reasons: changes in the porosity contents, oxidation rate of metallic powders and metallic oxide content in a various milling durations [19].

S.A. Sajjadi et al [10] used different particle sizes of alumina (20μ and 50 nm) to study the role and effect of those sizes on the aluminum (A356) matrix, which was produced by using stir casting method at different stirring speeds of (200, 300, 450) rpm. The author found that the best distribution of reinforcement in a composite microstructure resulted when the stirring speed was 300 rpm as the lower stirring speed of 200 rpm was not enough to fully disperse the Al_2O_3 particles. Furthermore, the higher stirring speed of 450 rpm caused more wastage of Al_2O_3 particles and formed more porosity because of more melt turbulence. Another finding from their study was that the wettability of the particles decreased by increasing the weight percent of reinforcement and decreasing the particle size due to increasing surface area and surface energy of nano particles. The hardness and porosity increased with increasing the amount of alumina percent and decreasing with the particle size. It was also found that the nanocomposite had

higher compressive strength than micro composite[11]. Researchers showed that the fabrication of aluminum and alumina composite up to 5wt% micron and 3wt.% nanocomposites did not form particles agglomeration[20].

- D. Özyürek et al demonstrated the effect of various amounts of volume percents of alumina (0.3 μm) which were as follows: (5, 10, 20 vol.%) on the wear properties of aluminum matrix (55μm). The composite was fabricated by using mechanical alloying method. Authors observed that the hardness increased with increasing the alumina content due to the homogeneous distribution and good interface between the alumina and aluminum matrix. On the other hand, wear rate reduced with increasing the alumina content and the sliding distance, while the Coefficient of friction decreased with increasing the Al_2O_3 content[21].
- Mazahery[22], found that the hardness increased as the amount of ceramic phase of alumina increased in the aluminum matrix, owing to the particle size in the form of nanoparticles which acts as an obstacle to dislocation motion. However, the highest hardness was observed with the volume percent of 2.5vol%. Furthermore, D. Özyürek conducted wear test at different loads to evaluate the role of alumina particles in aluminum matrix. They found that, the wear rate decreased with increasing the amount of alumina content and sliding distance due to higher load-bearing capacity of hard reinforcing material and good interfacial bond between the alumina particles and aluminum matrix [21].
- Nouari Saheb et al studied the effect of processing parameters of aluminum matrix reinforced with alumina (150 nm particle size) by mechanical alloying and SPS techniques. Author proved that, increasing the sintering time from 5min to 20 min decreases the hardness of the composite due to the grain growth. The increase in Al_2O_3 content to 10 vol.% contributed to decreasing the particle size, which led to the formation of more equiaxed particles. Further increase in alumina

content to 15vol.%, reduced the densification of the composite because of the consolidation of nanocomposites powders becomes more complicated at a higher fractions of ceramic nanoparticles. Author reported that 10vol% of alumina with the following SPS parameters (T: 550˚C, holding time: 5min, heating rate:200˚ C/min, and P: 50Mpa) are the best parameters to get a highest mechanical properties such as (hardness and tensile strength) [23].

- Yung-Chang Kanga, used different volume fractions of Al_2O_3 (50 nm particle size) to study the effect of volume fraction of alumina on the mechanical properties of aluminum matrix (28 μm particle size). Author used a powder metallurgy process route and CIP sintering in this study. It is reported that the grain size decreased as the particulate volume fraction increased, while the content of Al_2O_3 that exceeded 4 vol.%, did not change the grain size. The reason was attributed to the amount of nano-particulate on the grain boundary that had reached to the saturation level, and the effect of nano-particles on the grain boundary pinning had been diminished. When nano-particles content in the composites exceeded 4vol.%, the agglomeration reduced the effectiveness of nano-particulates[24].
- K. Dash used spark plasma sintering to reinforce different Al_2O_3 volume percents in the form of micro and nano particle sizes. Different volume percents of Al_2O_3 (0.5, 1, 3, 5, 7 volume %) were used with less than 50nm particle size. Alumina with the following volume percents also were used (1, 5, 20 volume%) with average particle size of 10 μm reinforced in (99.7% alumina). Spark plasma sintering technique was used under the following Parameters: (T:773K, P:50MPa, heating rate: 353k/min and a holding time of 5min). They discovered that, with the above parameters, the densification decreased with increasing the alumina content, because of the higher alumina content. Which in turn, increased the alumina-alumina contact resulting in impeding the deformability of aluminum particles. The hardness of nanocomposite increased up to 5 vol.% of

Al_2O_3 due to the positive effect of dispersion strengthening. Researcher proved that, further increasing in volume content results in decreasing the hardness of the composite due to the agglomeration of nanoparticles. The distribution of alumina in nanocomposites is reported to be better than in the micro composites. The agglomeration in the nanoparticles leads to less densification of nanocomposites. In contrast, the agglomeration associated with the micro composites did not impair the densification. This effect has been attributed to the specific surface of coarser particles which are lower and the powder compressibility are higher[25].

2.6 Graphene oxide properties

The unique physical, mechanical, and chemical properties of graphene will keep it an attractive candidate for many mechanical and tribological applications[5].

2.6.1 Thermal and electrical properties

Thermal properties are one of the key factors for better performance and reliability of the composite material especially in the electronic industry. The strong, anisotropic bonding and the low mass of the carbon atoms give the graphene unique thermal properties [7,37]. Hence, it has been heavily used in the research due to high thermal conductivity which reaches up to 5000w/m-k. Thereby, Graphene could be used to add an extra heat-resistance or conductivity to the plastics or other materials[7,8]. Material that conducts heat like graphene also will conduct electricity because both processes transport energy by electrons. The hexagonal lattice of graphene can offer little resistance to electrons, which pass through it easily, carrying electricity better than the superb conductor materials such as Copper[7]. Graphene and graphene based materials can be used as promising materials for thermal management. Therefore, several theoretical and experimental studies have been reported[39].

2.6.2 Mechanical properties of graphene oxide

The mechanical properties such as Young's modulus, strength, and stiffness are intrinsic properties for the composite material. Taylor [39] has observed that, increasing the oxide agent (O^-) and (OH^-) will lead to increase in the C-C bond length at each hexagonal lattice. The flat planes of carbon atoms in graphene which are as shown in Fig.(2.12) can relatively flex without breaking apart the atoms. Which in turn, will give high stiffness to the matrix[7].

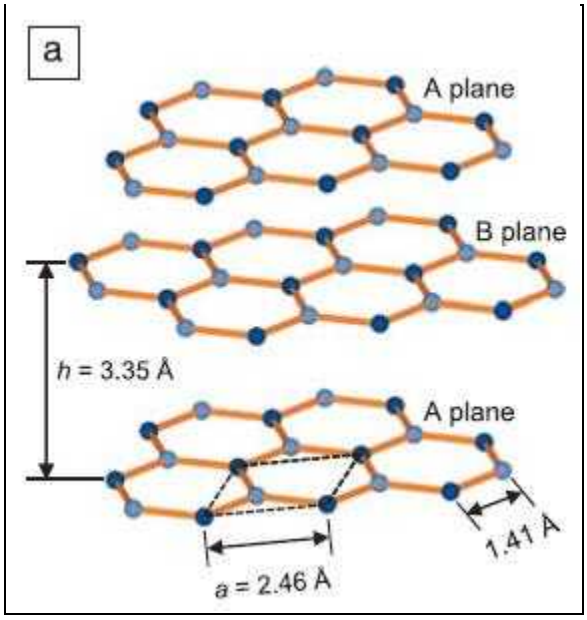

Figure 2.12 Schematic of the atomic arrangement in graphene sheet

2.7 Synthesis of aluminum (Al) and graphene oxide (GO)

- Wen-ming Tian et al sonicated different wt. % of GO as follows: (1, 3, 5 wt.%) in (7055) aluminum alloy by using an ultrasonic bath with acetone solution. Spark plasma sintering technique was used under the following parameters:

  (T: 400°C, dwell time:1min, P:50MPa and a heating rate: 50°C/min). It has been reported that severe agglomerations were observed for the GO content more than 1wt%. Thereby, physical

properties of graphene composite deteriorated due to weak interface between the reinforcements. Aluminum carbide (Al_4C_3) was not detected due to low sintering temp. It has been concluded by the author that at 1wt.% of graphene, the highest hardness and compressive strength were observed. Furthermore, the compressive strain decreased due to obstruction of dislocation and vacancies [26].

- Different milling times were employed at (10, 30, 60, 90 min) by Mina Bastwros et al to investigate the effect of milling time on the dispersion of 1wt% of graphene. Graphene was reinforced in aluminum (Al6061) composite by using hot compaction method, which was done in two stages: pre-compaction pressure of 50 MPa at room temperature, then at hot-pressed pressure of 100 MPa for 10 min at 630°C. The author found that, the alloy particles size increased with a longer milling times. However, the graphene particles size decreased as the milling time increased. However, the milling times of (10, 30min) were not long enough to fully disperse the graphene into aluminum 6061 matrix. The particles which have been milled for 10 min and 30 min in ball milling caused degradation for the mechanical properties. In addition, at milling time of 10min, presence of agglomeration was observed in the graphene which significantly weakening the composite to a point where the strength is less than the reference material. The graphene sample which was milled for 10 min shows a big crack in the fracture surface of composite due to poor interface between the large graphene cluster and the matrix phase, which act as a crack nucleation site. It has been proved that, as milling time increased to 60 min and 90 min, the flexural strengths significantly increased to 760 MPa and 800 MPa, respectively. The author observed no detection of aluminum carbide phase in his study [27].
- Andy Nieto et al [28] used the bulk graphene nanoplates in their study to explore the feasibility whether the graphene structure is retained at extreme processing conditions in SPS. The

consolidation was carried out at a pressure of 80 MPa, temperature at 1850°C, holding time at 10 min and a heating rate of 200°C/min in argon atmosphere. The author proved that the GNPs are successfully retained with a minimal damage. The density of starting GNP powder was measured and found to be 1.82 g/cm3. Whereas, the true density of the bulk GNP pellet was 2.11 g/cm3. The author reported that, increase in the density is largely attributed to the consolidation of powder. The top surface shows a higher hardness than the fracture surface and it was consistent with the amount of permanent deformation. As reported, GNPs can undergo sharp bends and form a corrugated-like structure. Author showed that the bending of GNP is responsible for the wrapping mechanisms around the grains that has been observed to impede crack propagation. Thereby, will lead to increase the toughness of the composites[28].

- Jingyue Wang et al. [29] synthesized 0.3wt% of GO in a pure aluminum matrix (99% purity). Aluminum flakes were added to the deionized water to form a powder slurry, the mixed slurry mechanically stirred until its color changed from brown to a transparent one. The GO/Al composite powders were heated to 550°C at a heating rate of 40 °C min. The study concluded that the composite with an addition of only 0.3 wt.% of GO exhibited a 62% improvement in the tensile strength as compared to unreinforced matrix.
- R. Pérez-Bustamante used different wt.% of GO as follows: (0.25, 0.50, 1.0 wt.%), which were reinforced into a pure aluminum matrix (99.9%). The composite was fabricated by mechanical alloying method with different milling times of (1, 3, 5h), the ball to powder weight ratio was maintained to be 5:1 and methanol medium was used as PCA. The composite was consolidated by cold compaction under a pressure of 950 MPa in argon atmosphere with different holding times as follows: (0.5, 1, 3, 5h), temperature was set at 500°C along with a heating rate of 5°C /min. It was showed that XRD reflections of carbon element are not present; this is attributed to the nano

metric size and the low content of the reinforcement phase which cannot be detected due to the detection limit of XRD. Raman spectroscopy showed that the intensity of the peaks was reduced as the milling time increased. This was reported due to increasing the amorphous fraction of the GNPs as a function of milling time. As the milling time increased, higher hardness values were observed. The author observed that in all the cases, higher hardness values obtained at 2 h of sintering and 5h of milling. Eventually, the author demonstrated that low GNP which was added into aluminum matrix is not enough to have more evident effect on the morphology, whereas the highest mechanical properties found to be at 1wt.% of GO [30].

- Muhammad Rashad et al. Sonicated 0.3wt% of graphene in acetone for 1 h to study the effect of GNP (5-15nm average thickness) on the mechanical properties of pure aluminum powder using mechanical agitator. The composite was compacted in SS mold under 170 MPA and sintered in a muffle furnace at 600°C for 6 h. The researcher found that, the density of pure aluminum decreased with addition of GNP since the density of GNP is less than pure aluminum. Thus, the density of composite reduced. The sintering process changed the composite dimensions owing to the shrinkage which affected the composite density. The author observed that, increasing the particle size leads to an increase in the porosity of the composite, because the GNP acts as a barrier for diffusion and rearrangement of particles. The author highlighted that the compressive strength of the composite is lower than the pure aluminum sample. In contrast, the tensile strength was improved by 11% than unreinforced aluminum matrix. The author attributed this increase in the tensile strength to the dimensional structure of graphene which contains long chains of C-C bonds, but under compressive strength the graphene is soft due to flake buckling which hinder the sample to squeeze. As reported, The yield strength and ultimate tensile strength for the composite found to be increased by 12% and 10%, respectively due to higher dislocation density

which leads to increase in the strength of the composite owing to smaller particles reinforcement [31].

- Sara Rengifo investigated the role of 2vol.% of GNPs (6–8 nm average thickness) in a pure aluminum with an average particle size of (2–10 μm). The mixture was Sonicated in acetone for 90 min. Thereafter, the mixture was dried in an oven for 24h at 75°C. The dried powder was sintered by spark plasma sintering (SPS) under the following parameters: T: 500°C, P: 50 MPa, heating rate: 50°C /min and a holding time of 10 min. The researcher found that, the density of pure aluminum sample was 96%, while the composite sample had a poor density of 91% due to the agglomeration of GNPs. The hardness of the composite sample had a lower density than pure aluminum sample by 7% due to the GNP has a tendency to agglomerate and restack, leading to form porosity in the composite. The author analyzed the samples by XRD analysis and he found that pure aluminum sample has a little formation of Al_2O_3. On top of that, The composite sample showed a formation of Al_2O_3 and Al4C3 phases. However, adding 2vol% of GNP to aluminum sample reduced the COF at room temp and high temperature. [32].
- Ravichandran et al used graphite and titanium dioxide in various amounts as fillers reinforced in aluminum matrix. Researchers found that, the grain size increased with addition of weight percent of graphite due to the agglomeration of the particles. In addition, the densification decreased with increasing the amount of hard material due to higher amount of fillers percentage [38] .
- Bisht et al applied a nano indentation test to measure the elastic modulus and hardness of the composites. Researcher indicated a less indentation depth for the sample with 1wt% graphene. while further increase in graphene content resulted in to high depth, indicating low hardness. The improvement in the hardness that reached up to 1wt% Graphene has been attributed to the

uniform distribution, resulting in sharing of the applied load transferred and providing high resistance to composite deformation. While reduction in the hardness values was attributed to graphene nano particle that created irregularities. These irregularities form stress concentration, which in turn, will create a porosity and make the interfacial bonds between the reinforcement and matrix weak [34].

2.8 Summary

Aluminum matrix nanocomposites have gained a lot of importance and attraction in the demanding applications due to high strength to weight ratio, effective cost and material abundance. It can be concluded from the extensive literature review that most of the synthesis being used in aluminum composite has been done on the hot and cold isostatic press sintering techniques with different mixing and sintering process parameters. Whereas, a few researchers have used spark plasma sintering technique in aluminum/graphene nanocomposites. Authors have performed various mechanical testing on the aluminum nanocomposite samples. Authors reported several challenges during the fabrication of the composites such as agglomeration, reaction of carbon with aluminum at elevated temperature forming aluminum carbide (Al_4C_3) which is detrimental to the mechanical properties, optimizing the weight percents of the used fillers which play a vital role in the mechanical properties of the composite. In addition, the researchers addressed and discussed the effect of particles size of different fillers and their influences on the microstructure of the composite.

As a conclusion, it has been noted that no study was found to develop aluminum hybrid nanocomposite reinforced with alumina and graphene oxide by using powder metallurgy techniques such a spark plasma sintering.

2.9 Significance of the study

As observed from the extensive literature review presented above, very few studies have been carried out in developing aluminum hybrid nanocomposites, whereby, two or more constituents have been added to the aluminum matrix. However, optimizing the optimum weight percent of each filler is a crucial factor in the hybrid aluminum nanocomposites in order to reach out to the highest mechanical and thermal properties. Hence, the present study focuses on developing the hybrid aluminum nanocomposites. Mechanical and thermal testing have been conducted to assess the performance of developed nanocomposites. Moreover, a range of characterization techniques have been used throughout the research phases to support various findings.

CHAPTER 3

EXPERIMENT PROCEDURES

3.1 Material

Aluminum powder with a purity of 99.5% is used as the matrix with a particle size of 30µm was produced from Alpha chemical company, Canada. Alpha alumina (Al_2O_3) powder was used as a reinforcement with 300 nm particle size and 99.8% purity with a surface area of 85 - 115 m^2/g, manufactured by union carbide corporation for BUEHLER Ltd, USA. Graphene oxide used as a second reinforcement which was procured from AD Nano Company, India, with the following specifications: purity ~99%, surface area 250 m^2/g. Specifications verified by X-ray fluorescence are as follows:

Table 3.1 Aluminum specifications

contents	Al	Si	Fe	Ti
%	>99.5	<0.25	<0.15	<0.25

Table 3.2 Alumina specifications

contents	Al_2O_3	SiO_2	P_2O_5	S	K_2O	TiO_2	V_2O_5	MnO
%	99.88	0.034	0.0085	0.026	0.027	0.0022	0.0041	0.0016

Table 3.3 Graphene oxide specifications

contents	C	O_2	other
%	77	22	1

3.2 Ultrasonication of alumina (Al_2O_3)

Before mixing the alumina powder with aluminum, alumina was sonicated for 10 min. to eliminate any agglomerations by using (ultrasonic prob sonicator, model: SONICS VCX 750) which shown in Fig. (3.1) under the following conditions: Room temperature, on and off ratio: 20 / 5s and amplitude: 35%. Different volume percents (10%, 20%, 30%) of alumina were sonicated under the same conditions.

3.3 Ultrasonication of graphene oxide (GO)

Before mixing the graphene oxide with the Al- X% Al_2O_3, it was sonicated in ethanol for 1 hour by using (ultrasonic prob sonicator, model: SONICS VCX 750, USA) which shown in Fig. (3.1) to exfoliate graphene oxide layers by pushing solvent molecules in between the layers, under the following conditions: Room temperature, on and off ratio: 20 / 5s and amplitude 35%. Different weight percents (0.25%, 0.5%, 1wt.%) of GO were sonicated under the same conditions.

Figure 3.1. Ultrasonic prob sonicator, model: Sonics Vcx 750, USA

3.4 Ball milling procedure

3.4.1 Al- Al_2O_3 powder mixing in ball milling

Pure aluminum with different Al_2O_3 volume percents (10% , 20%, 30%) were loaded in zirconia vial and mixed for 24 hour by using (high energy ball mix, model: HD/HDDM/01, Union process, Inc. USA) which is shown in Fig. (3.2) to produce a homogeneous mixture. The process was carried out under the flow of Argon gas (Ar) atmosphere to avoid oxidation. 50 ml of ethanol was used as a process control agent (PCA) to avoid excessive cold welding and agglomeration. Zirconium oxide (ZrO_2) balls were used (5mm dia.) with ball-to- powder weight ratio (BPR) of 10:1. Mixing was performed at a speed of 200 rpm. The milling experiment was halted after the first hour of the process to remove any powder from the walls of the vial to eliminate any accumulation of powder on the walls. The vials are purged with (Ar) during the whole mixing process. Subsequently, the powder mixture is dried in an oven at a temperature of 80˚C for 12 hours.

Figure 3.2 High energy ball mix, model: HD/HDDM/01, union process, Inc. USA

Table 3.4 Summary of mixing process parameters for Al- Al_2O_3 nanocomposites

Samples	Speed rpm	BPR	Mixing time	PCA	Atmosphere
Al-10 vol.% Al_2O_3	200	10:1	24 h	ethanol	argon
Al-20 vol.% Al_2O_3					
Al-30 vol.% Al_2O_3					

3.4.2 Al-Al_2O_3-GO powder mixing in ball milling

The mixed powder of Al-10 vol% of Al_2O_3 (the optimum volume % found from phase-2 of our work) was added to different weight percents of GO (0.25%, 0.5%, 1%) and mixed again in high energy ball mixer for 24h. As earlier, the process was carried out under the flow of argon gas (Ar) atmosphere to avoid oxidation. 50 ml of ethanol was used as process control agent (PCA) to avoid excessive cold welding and agglomeration. Zirconium oxide (ZrO_2) balls were used (5mm dia.) with ball-to- powder weight ratio (BPR) of 10:1. Mixing was performed at a speed of 200 rpm. The milling experiment was halted after the first hour of the process to remove any powder from the walls of the vial to eliminate any accumulation of powder on the walls. The vials are purged with (Ar) during the whole mixing process. Subsequently, the powder mixture is dried in an oven at a temperature of 80˚C for 12 hours.

Table 3.5 Summary of mixing process parameters for Al- Al_2O_3 -GO hybrid nanocomposites

Samples	Speed (rpm)	BPR	Mixing time(h)	PCA	Atmosphere
Al-10% Al_2O_3-0.25%GO	200	10:1	48h	ethanol	argon
Al-10% Al_2O_3-0.5%GO					
Al-10% Al_2O_3-1%GO					

3.5 Spark plasma sintering (SPS)

3.5.1 Sintering process for Al-Al_2O_3 nanocomposites

As received aluminum powder was used to fabricate a reference sample. Aluminum powder was charged in a 20 mm graphite die as shown in Figure (3.4). Graphite sheet approximately 0.35 mm was placed in between the die and the powder as well as between the powder and the punch, to easily remove the sample and avoid the wear of the punch. Spark plasma sintering machine from FCT group, system GMBH, Germany, as shown in Figure (3.5), was used to sinter the aluminum and the Al-X% Al_2O_3 composite samples. The sintering parameters used were as shown in the Table (3.6). Three different composite samples containing different volume percents of alumina (10% , 20%, 30% Al_2O_3) were sintered under the same conditions. The process flow diagram in Fig (3.3) was used for the whole sintering processes.

Table 3.6 Summary of sintering process parameters for Al/ Al-Al_2O_3 nanocomposites

Samples	Temperature (°C)	Pressure (Mpa)	Holding time (min.)	Heating rate (°C/min)
Al	550	50	10	200
Al- 10% Al_2O_3				
Al- 20% Al_2O_3				
Al+-30% Al_2O_3				

3.5.2 Sintering process for Al- 10%Al_2O_3-GO nanocomposites

Spark plasma sintering machine from FCT group, system GMBH, Germany, as shown in Figure (3.5), was used to sinter the (Al-10vol%Al_2O_3-X%GO) hybrid nanocomposite samples. The hybrid mixed powder was charged in a 20 mm graphite die as shown in Figure (3.4). Graphite

sheet approximately 0.35 mm was placed in between the die and the powder as well as between the powder and the punch, to easily remove the sample and avoid the wear of the punch. The sintering parameters used were as shown in the Table (3.7). Three different hybrid nanocomposite samples containing different wt.% of GO (0.25%, 0.5%, 1% GO) were sintered under the same parameters and conditions. The process flow diagram in Fig (3.3) was used for the whole sintering processes.

Table 3.7 Summary of sintering process parameters for Al-10% Al_2O_3- GO nanocomposites

Samples	Temperature (°C)	Pressure (MPa)	Holding time (min.)	Heating rate (°C/min)
Al-10% Al_2O_3-0.25%GO	550	50	10	200
Al-10% Al_2O_3-0.5%GO				
Al-10% Al_2O_3-1%GO				

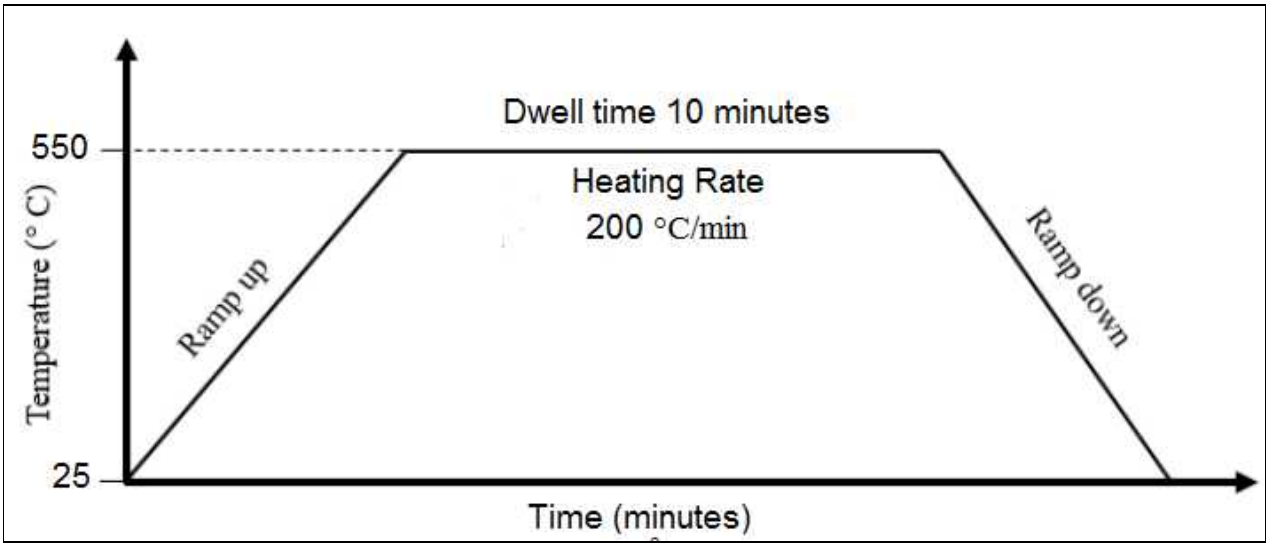

Figure 3.3 Process flow of spark plasma sintering (SPS)

Figure 3.4. Graphite die

Figure 3.5. FCT group, system GMBH SPS.

3.6 Mounting and grinding

The sintered samples (20 mm dia.) were mounted by using (Qualitest, hot mounting press, USA) Fig (3.6) and grounded using different grit of papers starting from rougher to finer grit (240, 320, 400, 600, 800, 1200). Afterward, the samples were polished with 0.3μm alumina paste as shown in Fig. (3.7) to obtain a polished samples as shown in Fig. (3.8)

Figure 3.6. Qualitest mounting machine

Figure 3.7. Grinding machine

Figure 3.8. Mounted/Grinded/Polished sample

3.7 Ultrasonic cleaning

After polishing, samples were cleaned with ethanol using an ultrasonic device for around 10 min. to remove any polishing debris remaining on the sample surface.

3.8 Density measurements

The density of sintered samples were measured according to the Archimedes principal and the rule of mixture by using (kern ABT weighing scale, 320g capacity, UK). The relative density of the nanocomposite materials were measured as the ratio of the measured to the theoretical value, whereby the theoretical density was calculated by rule of mixture.

Rule of mixture is a method of approach to estimate the properties of composite material, based on an assumption that a composite property is the volume weighed average of the phases (matrix and dispersed phase)

$$\mathbf{d_c = d_m * V_m + d_f * V_f}$$

where, d_c is a density of composite, d_m is a density of matrix, d_f is a density of dispersed phase. V_m is a volume fraction of matrix, and v_f is a volume fraction of dispersed phase.

Archimedes principle state that any object totally or partially immersed in a fluid buoyed up by a force equal to the weight of the fluid displaced by the object.

weight of displaced fluid = weight of object in vacuum – weight of object in fluid

Figure 3.9 Kern ABT weighing scale, 320g capacity, UK.

3.9 Hardness measurements

Vickers hardness test was performed on the sintered samples by using a Zwick Roell, Germany Vickers machine shown in Fig. (3.10). The Vickers indenter which made of diamond in the form of square –base pyramid having an angle of 136˚ between faces was used at a constant load of 500 gf for 10 s. An average of 10 readings were taken for each sintered sample and the average is reported.

The Vickers hardness number was calculated according to the formula:

$$\text{VHN} = 2P\sin\left(\frac{\theta}{2}\right)/d^2 = \frac{1.854P}{d^2}$$

where, P is the applied load in (kg), ɵ is the indenter face angle of 136˚, d is the mean diagonal length in mm and 1.854 is a constant which incorporate conversion factors to give a unit of VHN a unit of kg/mm^2

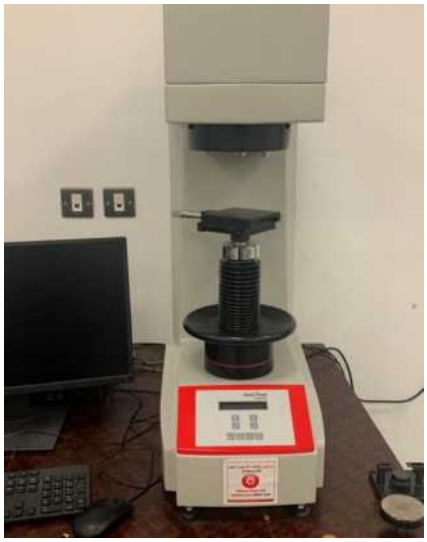

Figure 3.10. ZWICK ROELL, Germany Vickers machine

3.10 Scanning electron microscope (SEM)

SEM is used to study the morphology of as received materials, the developed mixtures and sintered samples, whereby, the electrons in the beam interact with the sample, producing various signals (secondary electron and backscattered electron) by scanning the surface with focused beam of electrons. These signals can be used to get an information about surface topography and composition. The SEM characterization performed in Quanta FEG 250,Thermo fisher company, USA. The samples were placed at a working distance of approximately 6mm and scanned at acceleration voltage up to 20 kv. Different magnifications were taken to focus the beam to a spot. Energy dispersive x-ray spectroscopy (EDS) detector was used conjunction with scanning electron microscope (Quanta FEG 250) to characterize the chemical composition of the sample . Figure (3.11).

Figure 3.11. Quanta FEG 250 scanning electron microscope with EDS detector.

3.11 X-ray diffractometer

X-ray diffraction is one of the primary analytical technique used for phase identification of crystalline materials which can provide a unit cell dimensions. By scanning the sample through a range of 2θ angles, the interaction of the incident rays with the sample produces constructive interference (and a diffracted ray) when conditions satisfy Bragg's Law ($n\lambda=2d \sin \theta$). Where n represents the order of diffraction, λ is the wavelength of x-ray source, d represents the inter-planar spacing and 2θ represents the diffraction angle. X-ray is produced by high speed electron accelerated by high voltage field bombarding the metal target. The detector records the number of x-rays observed at each angle 2θ and convert it into peaks. The powder diffractograph carried out on a Rigaku miniflex x-ray diffractometer as shown in Fig (3.12) using Cu Kα radiation with a wavelength 0f 1.5416A and an acceleration voltage of 30kv at a scanning speed of 3˚/min.

Figure 3.12. Rigaku miniflex x-ray diffractometer.

3.12 Raman spectroscopy

Raman spectroscopy is a spectroscopic technique that is known as vibrational technique, which is extremely sensitive to geometric structure and bonding within molecules. Raman effect is based on inelastic light scattering at the chemical bonds of sample due to vibrations in the chemical bonds, this interaction causes a specific energy shift in parts of the back scattered light which results in unique Raman spectrum. Raman spectroscopy is unique finger print of material, where it can provide a useful information about the peak intensity which reflect the quantity of the compound, peak shift which predict the stress-strain state and peak width can estimate the degree of crystallinity. The experiment conducted by using Nicolet NXR FT-Raman Spectrometer, Thermo fisher, USA. Pure graphene oxide powder has been tested as a reference sample. And 10mg of composite mixture which containing GO has been tested.

Figure 3.13. Nicolet NXR FT-Raman spectrometer, Thermo fisher, USA

.

3.13 Compression test

Compression test is one of the mechanical testing methods used to determine the behavior or response of a material while exposed to compressive loads by measuring stress, strain, elastic modulus to determine whether the material is suitable for the intended application or not. The experiment was carried out on a compression platens, Instron, model: 3367, USA. as shown in Fig.(3.14). The samples size prepared according to ASTM E9-89a standard by using an electric discharge machining (EDM), whereby the samples are maintained at length to diameter ratio of (1.5). An average of 3 tests for each composition were conducted at a constant compression rate of 0.3mm/min.

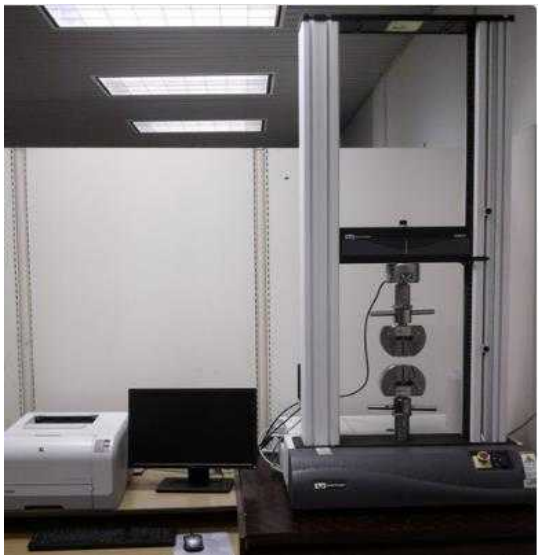

Figure 3.14 Compression platens, instron, model: 3367

3.14 Differential scanning calorimetry (DSC)

DSC is a thermal analysis technique which studies the thermal properties of materials as with a function of temperature/ time conditions, while the calorimetery measure the heat flow. DSC relies on the measurement of the difference between the heat flow vs. temperature relation of the sample and the heat flow vs. temperature relation of a standard. There are two different conventions: endothermic and exothermic reaction which can be expressed with the help of positive or negative peaks based on the experimental conditions. Differential Scanning Calorimetry (DSC) measurements were recorded to study phase transitions, exothermic and endothermic decompositions taking place in the samples. The experiment conducted on the NETZSCH STA 449F3 Jupiter, Germany instrument Fig.(3.15). First, DSC instrument calibrated by using empty aluminum pan to make sure the baseline is having accurate reading. whereby, an empty aluminum pan was used as reference. The pure aluminum and composite samples (6mg) were placed in platinum crucible with Al_2O_3 liners and compressed in non-hermetic pan. The

samples were heated from room temperature to 720˚C at a heating rate of 10 ˚C /min under argon atmosphere (flow rate of argon gas, 50 ml/min). Subsequently, all the samples were cooled at a rate of 10 ˚C /min to ambient temperature.

Figure 3.15 NETZSCH STA 449F3 Jupiter, Germany instrument.

3.15 Thermal expansion

Thermal expansion is the tendency of material to change its shape, area and volume in response to change in temperature. There are three ways to classify the thermal expansion:

Linear expansion, superficial expansion and cubical expansion. In the thermal expansion, the material is exposed to heat at a given temperature. Thus, the molecules begin to separate causing expanding the substance. In this experiment the Mettler Toledo instrument (TMA/SDTA LF/100) shown in Fig. (3.16) was used to study the coefficient of thermal expansion of pure aluminum and the nanocomposite samples. Smooth surface cubic samples were prepared in dimensions of approximately (2x2x2)mm .The experiment was carried out from room temperature up to 350˚C with a heating rate of 10 ˚C/min.

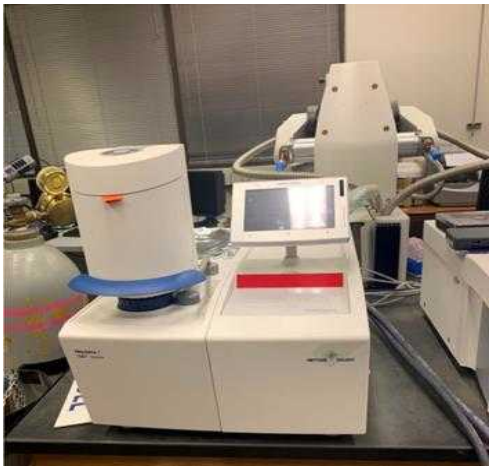

Figure 3.16 Mettler toledo instrument (TMA/SDTA LF/100)

3.16 Conversion for the used fillers quantity

Alumina contents in the nanocomposites (Al-X% Al_2O_3) is calculated in a form of volume percent since most of the literatures used volume percent to easily quantifying the used quantity whereas, it is used weight percent for GO content associated with the hybrid nanocomposite (Al-10vol% Al_2O_3-X wt. %GO) as the researchers were used wt.% with the GO. The conversion Table (3.8) shows the conversion of used quantity in volume and weight percents.

Table 3.8 Shows the conversion from volume to weight percent.

Samples	Density of Al_2O_3 (g/cm^3)	Density of Al (g/cm^3)	wt. percent %
Al-10 vol.% Al_2O_3	3.95	2.7	13.98
Al-20 vol.% Al_2O_3			26.78
Al-30 vol.% Al_2O_3			38.54

CHAPTER 4

RESULTS AND DISCUSSIONS

4.1Results for phase I

The results for the phase I are concerned with the characterization of the as received powders for aluminum, alumina and graphene oxide materials. Furthermore, hardness and density tests which are conducted for the developed aluminum and Al-X%Al_2O_3 nanocomposites will be presented. A detailed characterization analysis of the dispersed mixture and sintered samples were investigated and the results will be presented.

4.1.1 SEM and XRD analysis of as received powders

The morphology of the as received powders was analyzed by scanning electron microscopy (SEM), X-ray diffraction (XRD) was also conducted to determine the various material phases of the as received powders. XRD was carried out on a Rigaku Miniflex X-ray diffractometer, using Cu Kα radiation (Y= 0.15416 nm) in the 2θ range 5˚- 120˚ at a scanning speed of 3˚/min.

Figure 1 (a – c) shows the high magnification SEM images of as received aluminum powder, Al_2O_3 and GO respectively. It can be observed from Fig. 1(a) that aluminum particles are spherically shaped with an average diameter of 30 microns. Fig. 1(b) shows the Al_2O_3 particles that are acicular with agglomeration in some areas. Whereas, Fig. 1(c) shows small sheets of graphene Oxide.

The XRD spectrums for all the as received powders are shown in Fig. 1(d – f). It can be seen from all these Figures that the XRD spectrums showed the signature peaks for the as received aluminum, alumina and GO powders.

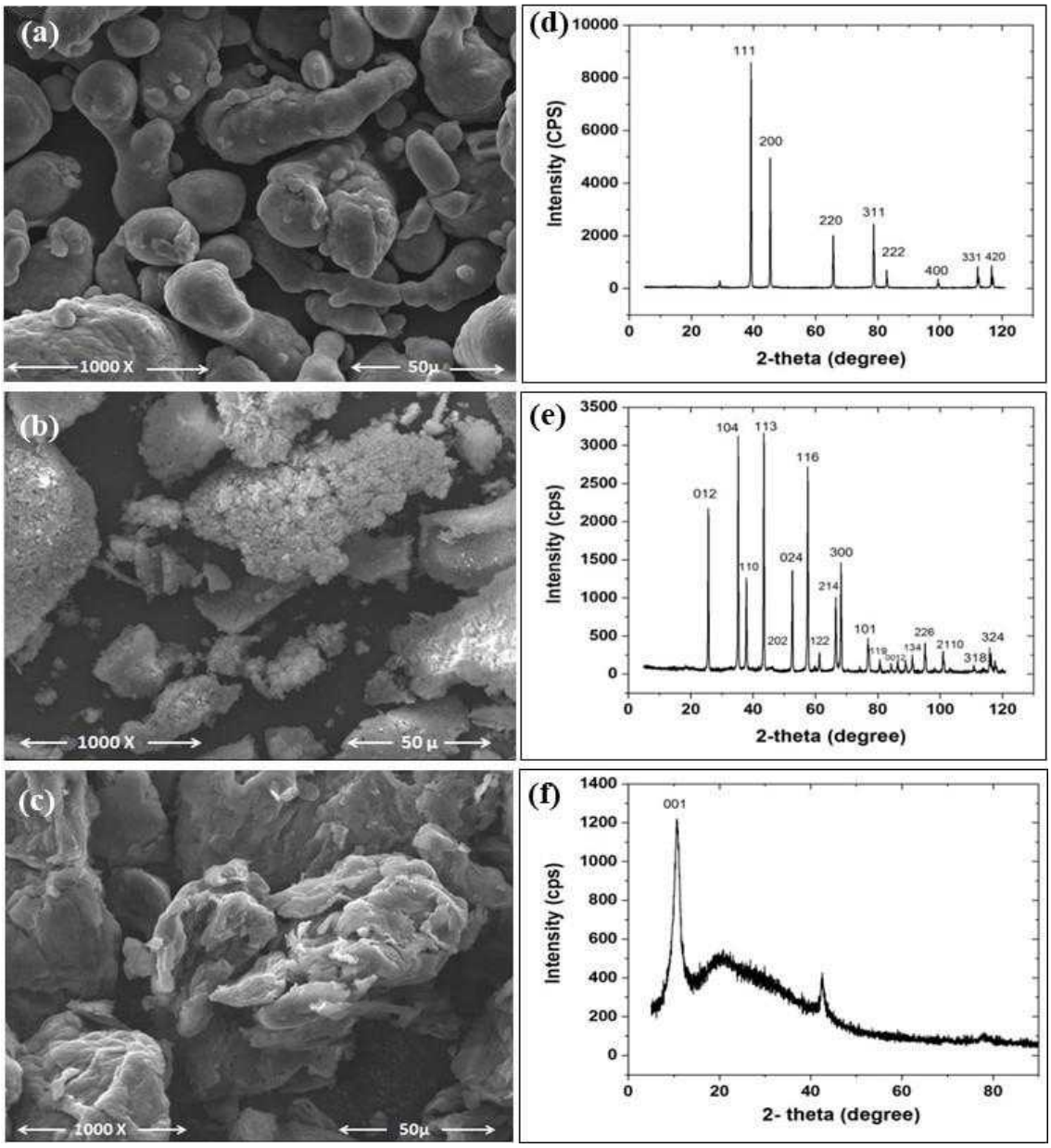

Figure 4.1: (a – c) SEM for as received powder of **a)** Al, **b)** Al_2O_3, **c)** GO. **(d – f)** XRD for the as received powders of **d)** Al, **e)** Al_2O_3, **f)** GO

4.1.2 SEM analysis of the Al-X%Al_2O_3 nanocomposite powders after mixing

The morphology of the nanocomposite powders of aluminum mixed with different volume percents of Al_2O_3 after ball milling was evaluated by SEM as illustrated in Fig 4.2 (a-c). It can be observed that in all the nanocomposite powders, the particles deformed from spherical shape into relatively irregular shape due to the effect of ball milling because of the collisions between the balls and the powder particles . It can be observed from Fig. 4.2 (a) that in Al-10% Al_2O_3, the nano particles of Al_2O_3 are uniformly distributed, whereas in Al-20%Al_2O_3 and Al-30% Al_2O_3 it can be observed that, alumina particles are non-uniformly distributed with a significant amount of agglomerations. The agglomerations tend to increase as the volume content of alumina increased from 20% to 30% Al_2O_3, respectively. Therefore, the reducing the agglomerations would be a key element of improving the mechanical properties of Al- (20% and 30 % Al_2O_3) nanocomposites due to restriction of interfacial area between the matrix and the reinforcement.

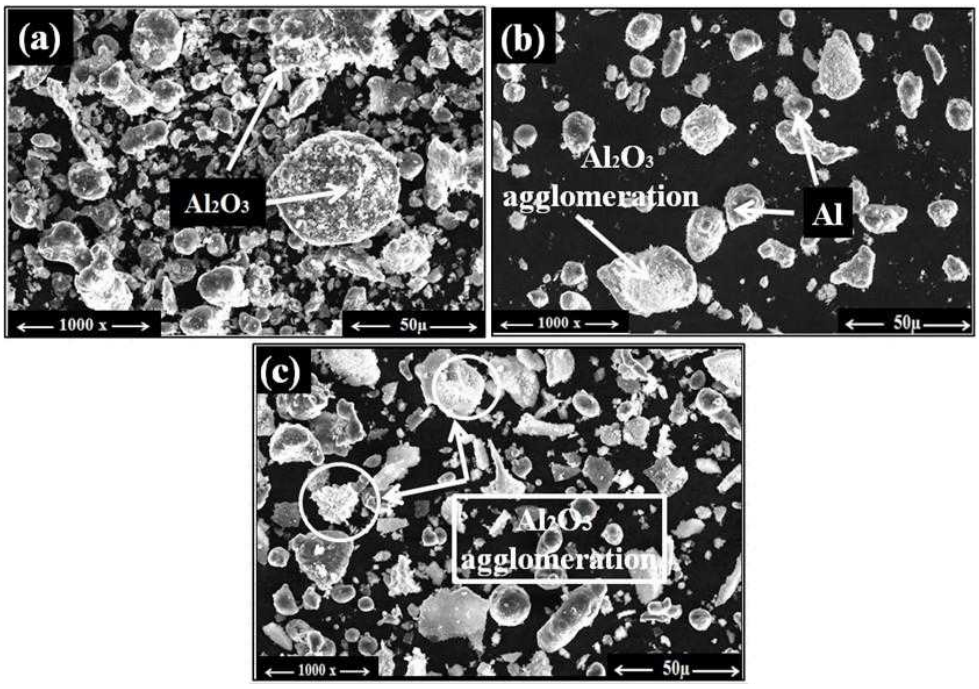

Figure 4.2. SEM after mixing **a)** 10% vol Al_2O_3, **b)** 20% vol Al_2O_3, **c)**. 30% vol Al_2O_3

4.1.3 Microstructure of (Al-X%Al_2O_3) nanocomposite samples after SPS

Figure 4.3(a), shows the SEM image for the SPS sample of Al-10% Al_2O_3 nanocomposite, where little porosity can be observed with a fine grain size. Adding more amount of alumina as in the Al-20%Al_2O_3 sample results in agglomerations of alumina in the aluminum grains as illustrated in the Fig 4.2 (b). A few cracks are also observed around the grains boundaries of the sample containing 20%Al_2O_3 . This can be attributed to a higher volume percent of Al_2O_3 content which makes the material brittle. Therefore, due to the brittleness of the sample which is associated with an increase in the volume percent of alumina, the fracture rate of the sample increased as was observed with Al – 30% vol. Al_2O_3 which fractured during the grinding and polishing of the sample. Hence, the SEM could not be taken owing to the difficulty faced during the grinding and polishing.

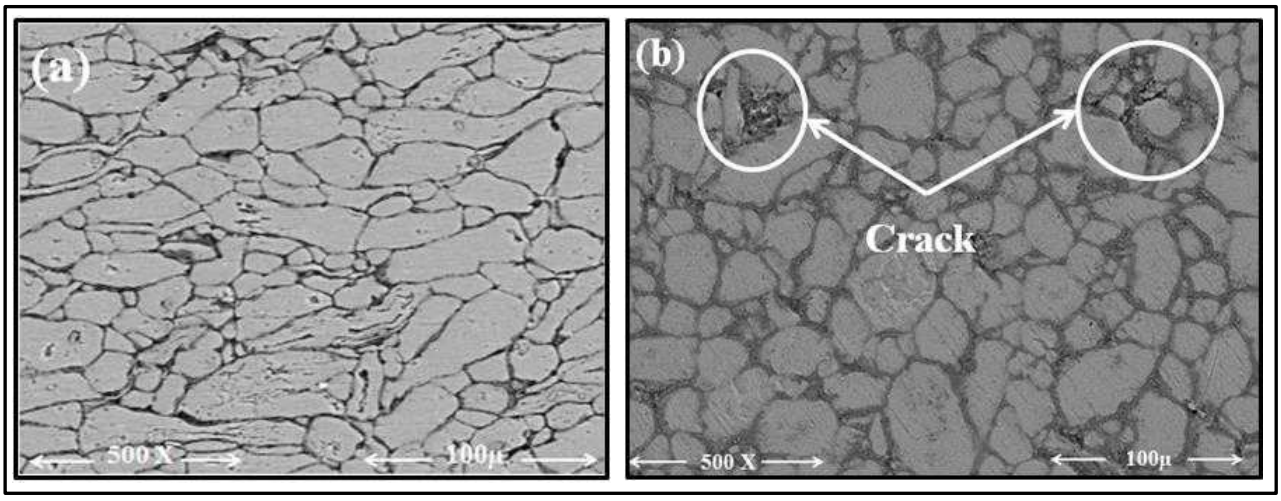

Figure 4.3 SEM after SPS. **a)** Al-10% Al_2O_3. **b)** Al-20% Al_2O_3

4.1.4 Density measurements of Al-X%Al_2O_3 nanocomposites

After sintering and grinding of the Al-X%Al_2O_3 nanocomposite samples, the experimental density was measured based on the Archimedes method and the results are as shown in Fig.(4.4). It is observed that pure aluminum showed a higher density of 99.7 % as compared to the nanocomposite samples. Among the nanocomposites, an increase in the volume percent of alumina resulted in a reduction in density as 10% of Al_2O_3 showed a density of 97.5% which reduced to 93.7 % as the volume percent increased to 20%. This is attributed to the reduction in the wettability between the alumina and the aluminum matrix because of the agglomerations resulting from the high volume content of alumina in the matrix. However, for the sample containing 30% of alumina, the density could not be measured because of the challenges mentioned above. Theoretical and relative density presented in Table (4.1).

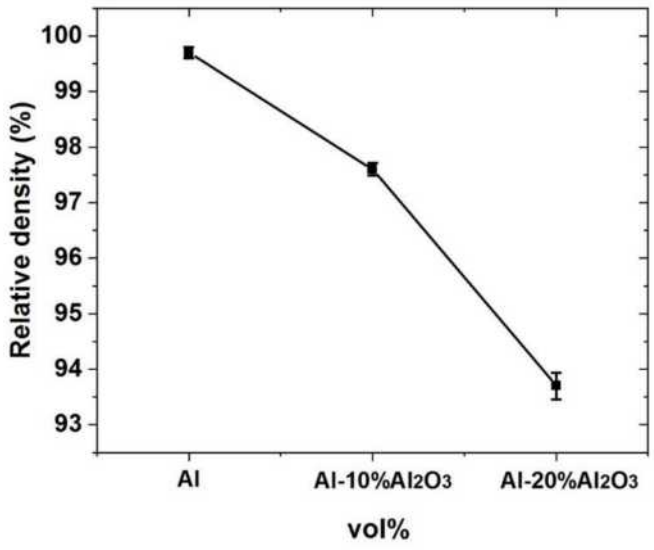

Figure 4.4 Relative density for Al, Al-10% Al_2O_3, Al-20% Al_2O_3

Table 4.1 Theoretical and relative density for Al, Al-Al_2O_3 nanocomposites

Density	Al	Al-10%Al_2O_3	Al-20%Al_2O_3
Theoretical density (g/cm^3)	2.70	2.78	2.88
Relative density (%)	99.7	97.5	93.7

4.1.5 Hardness measurements of Al-X%Al_2O_3 nanocomposites

Figure 4.5 shows the hardness results of the sintered samples of Al-X% Al_2O_3 nanocomposite. Sintered pure aluminum sample showed a Vickers hardness value of 32 HV. However, on addition of 10% of Al_2O_3 resulted in a significant increase in the hardness from 32 to 55.8 HV. This tremendous increase in the 10% Al_2O_3 nanocomposite hardness can be attributed to the presence of the uniformly distributed hard and non-deformable nano particles of Al_2O_3 particles within the aluminum matrix as can be seen in Figure 4.2(a) . The presence of these particles thereby, hinder the movement of dislocations, resulting in the increase in the hardness. Further increasing the amount of alumina to 20% results in a reduction in the hardness from 55.8 to 47.2 HV. This reduction can be attributed to the lower densification that was triggered by the agglomeration of Al_2O_3 particles, which was clearly observed in the SEM images 4.2 (b) and (c) owing to high volume percent and non-uniform distribution of Al_2O_3. As mentioned earlier, with a further increase in the volume percent of alumina to 30%, the nanocomposite sample fractured due to an increased brittleness resulting from the agglomerations and cracks during sintering, due to which the hardness measurements were not done.

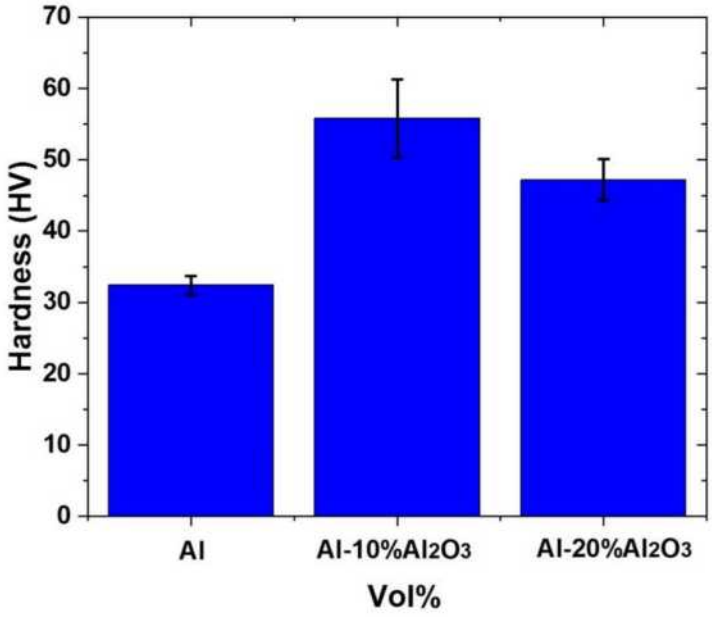

Figure 4.5 Hardness results for Al, Al-10% Al_2O_3, Al-20% Al_2O_3

4.1.6 Summary of Phase I

Based on the above results, Al-10 vol%Al_2O_3 nanocomposite showed the highest hardness, reasonable density and uniform distribution of Al_2O_3 particles in the aluminum matrix among all the other developed nanocomposites. Hence, 10 vol% Al_2O_3 was selected as a first filler to fabricate the aluminum hybrid nanocomposite.

4.2 Results from Phase II

In this phase, aluminum hybrid nanocomposites are fabricated by reinforcing the Al-10 vol%Al_2O_3 with different weight percents (0.25, 0.5 and 1 wt%) of GO. A detailed characterization analysis of the dispersed hybrid nanocomposite powders and the sintered samples will be presented.

4.2.1 SEM after mixing for (Al-10%Al_2O_3-X%GO) hybrid nanocomposites

Figures 4.6 (a-c) represents the morphology of the mixed powders for the developed Al-10% Al_2O_3- X%GO hybrid nanocomposite samples. A uniform distribution of GO can be observed for the Al-10% Al_2O_3- 0.25%GO hybrid powders. It can be observed that in all developed hybrid samples shown in Figure (4.6), Al_2O_3 is tending to be distributed inside the grains while the GO distributed along the grain boundaries.

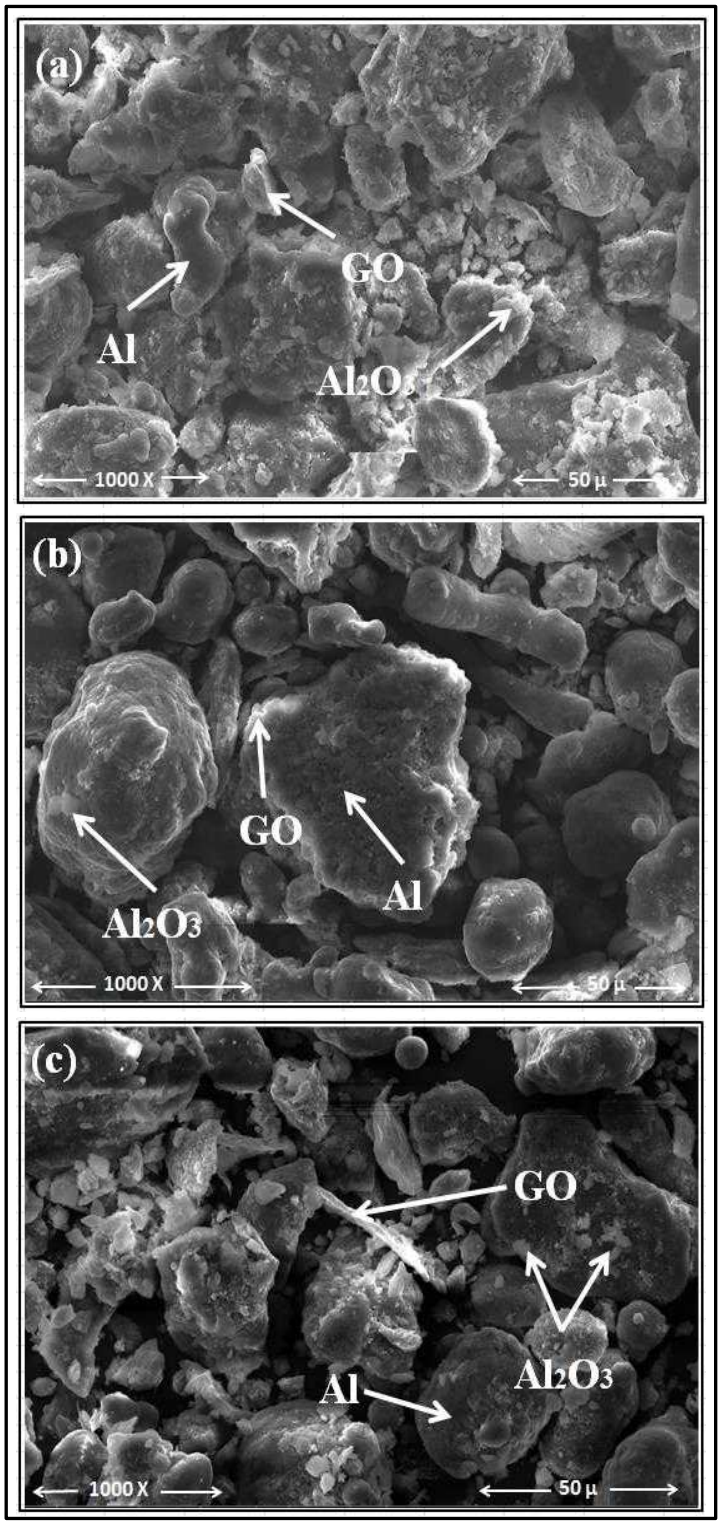

Figure 4.6 SEM after mixing for **a)** Al-10% Al_2O_3-0.25% GO. **b)** Al-10% Al_2O_3-0.5% GO. **c)** Al-10% Al_2O_3-1%GO

4.2.2 Microstructure of Al-10%Al_2O_3-X%GO hybrid nanocomposites

The microstructure of the developed hybrid nanocomposite was investigated by SEM as presented in Fig(4.7). A uniform distribution of GO along the grain boundaries is observed in the sample containing 0.25wt.% GO, whereas, in the samples containing 0.5wt% and 1wt% of GO some agglomerations of graphene oxide were observed as highlighted in Fig. (4.7). Another observation noted from the Figures was the presence of porosity which is associated with the sample containing 1wt% of GO. It can also be observed that the grains in the samples containing 0.25% and 0.5% of GO are finer as compared to the sample containing 1wt% of GO, in which relatively larger grains are observed. Figure 4.7(d) shows the results of EDS that was conducted on the Al-10%Al_2O_3-0.25% GO hybrid nanocomposite sample to investigate the distribution of each of the fillers. The concentration of each of the fillers is presented in Table (4.2). The higher concentration of alumina was found inside the aluminum grains, while the concentration of graphene oxide was found to be along the grain boundaries. Hence, increasing the amount of GO tends to increase the porosity resulting due to the GO agglomeration along the grain boundaries, thereby, hampering the densification process.

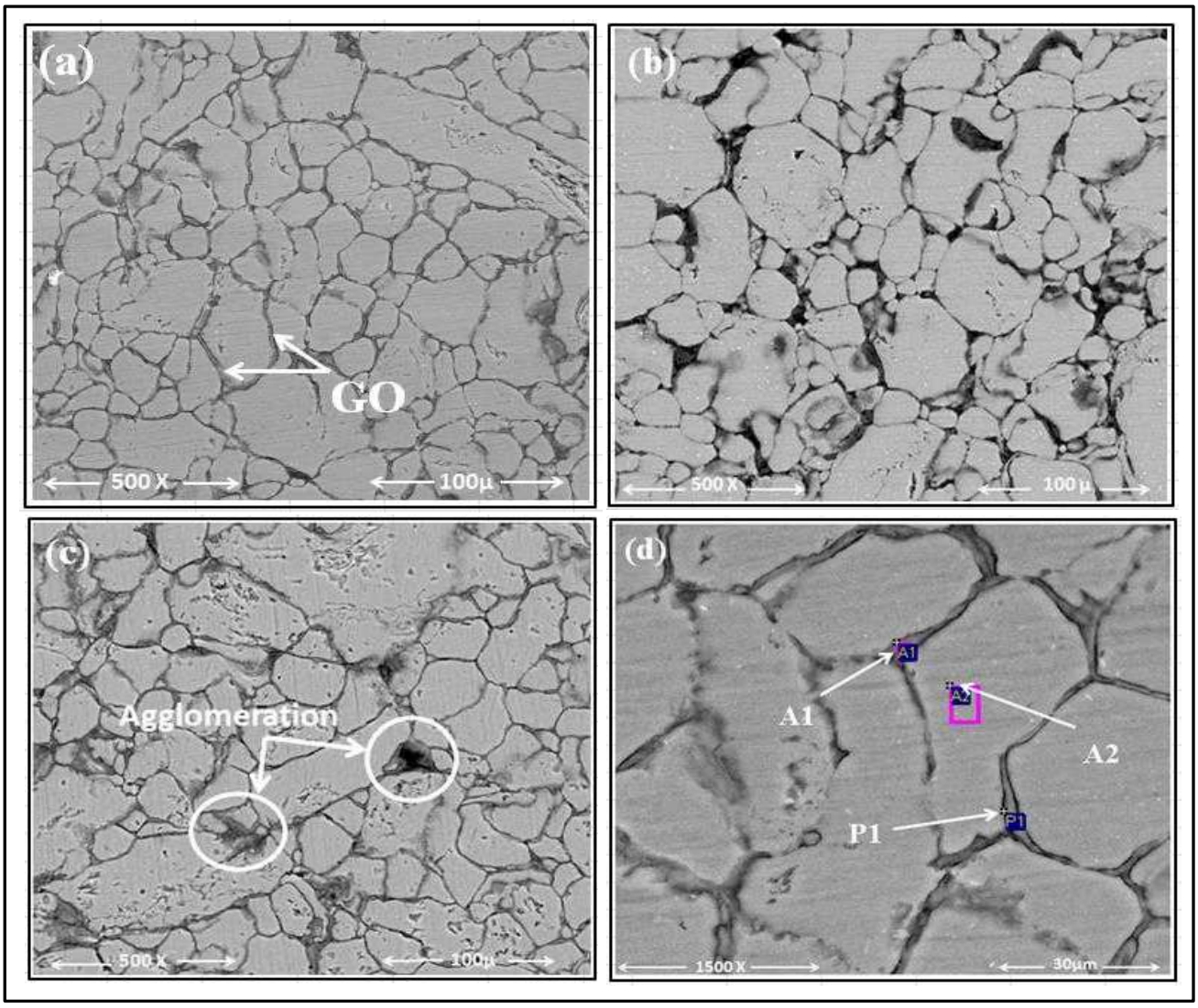

Figure 4.7 SEM of SPS samples **a)** Al-10% Al_2O_3-0.25% GO **b)** 10% Al_2O_3-0.5% GO **c)** 10% Al_2O_3-1 % GO **d)** EDS analysis for the hybrid composite sample (Al-10% Al_2O_3-0.25%GO)

Table 4.2 EDS analysis for the optimum hybrid sample (Al-10% Al_2O_3-0.25%GO).

Spectrum	Al	C	O	Total
A 1	92.60	6.04	1.36	100
P 1	94.39	3.07	2.54	100
A 2	81.83	5.98	12.19	100

4.2.3 Density measurements of Al-10%Al_2O_3-X%GO hybrid nanocomposites

After sintering and grinding/polishing of Al-10%Al_2O_3-X wt.% GO hybrid nanocomposite samples, the experimental density was measured based on the Archimedes method and the results are as shown in Fig(4.8). The results show that the relative density is reduced with increasing GO content, whereby, adding 0.25 wt. % of GO to the Al-10% Al_2O_3 nanocomposite is decreases the relative density from 97.5% to 96.8 %. Further addition of graphene oxide to Al-10% Al_2O_3 nanocomposite gradually reduced the relative density to 95.4% and 94.6% corresponding to 0.5wt% and 1wt% GO reinforcements, respectively. This reduction in the density is attributed to the tendency of graphene oxide to distribute itself along the grain boundaries which impedes the densification process, consequently, resulting in higher porosity with a higher content of GO as observed in SEM images in Fig (4.7).

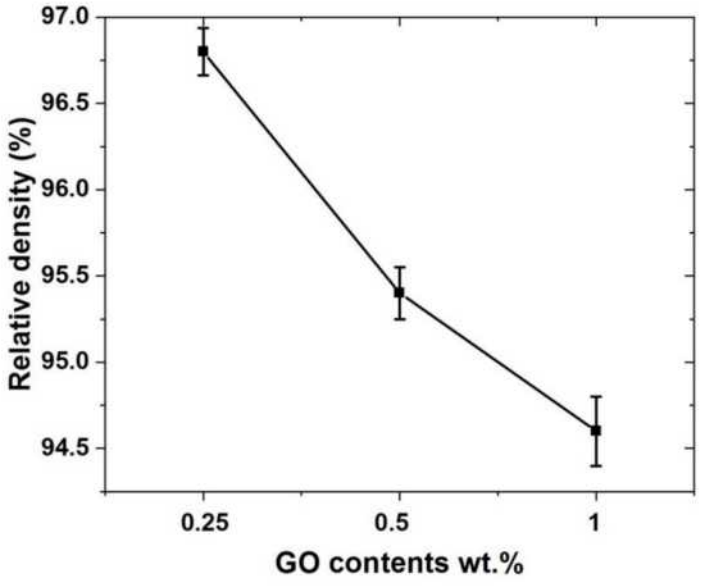

Figure 4.8 Relative density for Al-10%Al_2O_3-X% GO hybrid nanocomposite

Table 4.3 Theoretical and relative density for aluminum hybrid nanocomposites

Density	Al-10%Al_2O_3-0.25%GO	Al-10%Al_2O_3-0.5%GO	Al-20%Al_2O_3-1%GO
Theoretical density (g/cm^3)	2.785	2.784	2.778
Relative density(%)	96.86	95.49	94.65

4.2.4 Hardness measurements of Al-10%Al_2O_3-X%GO hybrid nanocomposites

The hardness results of Al-10% Al_2O_3-X% GO are presented in Fig. (4.9). The highest hardness of 63 HV was observed for the hybrid sample containing 0.25wt.% of GO among all the developed samples. The hardness reduced to 57HV with an increase in the GO content to 0.5wt%. However, not much difference was observed in the hardness of the hybrid sample with a further increase in the GO content to 1wt%. The increase the hardness of the hybrid nanocomposite with a low content of GO (0.25 wt.%) is attributed to the uniform distribution of both the fillers, Al_2O_3 and GO in the matrix. The homogeneous distribution of these fillers help in the load transfer from the matrix leading to a higher hardness of the hybrid nanocomposite. Furthermore, these fillers as discussed above and shown by SEM influences the microstructure of the hybrid nanocomposites resulting in finer the grain size. All these factors, enhance the bonding between the matrix and the fillers. The reason for observing lower hardness in the samples containing 0.5wt% and 1wt.% as compared to 0.25wt% GO sample is attributed to the larger grain size as observed in Fig (4.7) due to less densification associated with the agglomeration and porosity.

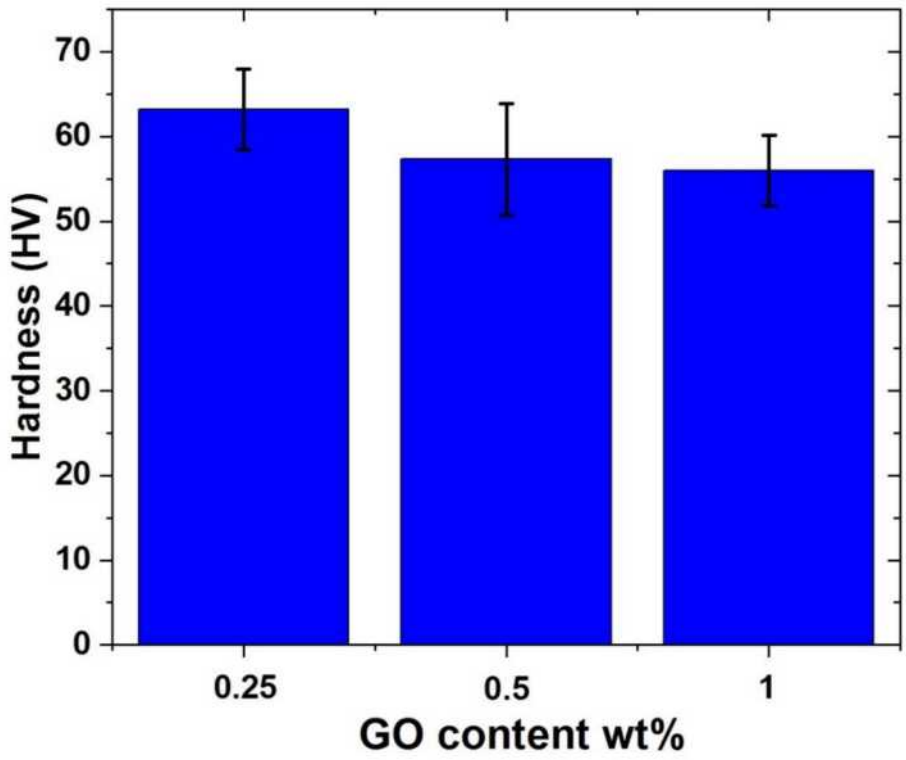

Figure 4.9 Hardness results for **(**Al-10% Al_2O_3- X% GO) hybrid nanocomposites

4.2.5 Raman spectroscopy of Al-10%Al_2O_3-X%GO hybrid nanocomposite powders

Fig (4.11) shows Raman spectra of GO powder and the hybrid nanocomposite powders after mixing. It can be observed that GO shows the two signature peaks/ bands one at approximately 1580 Cm^{-1} corresponding to the G band resulting from the stretching of the C-C bond in GO , and an another one at approximately 1350 Cm^{-1} corresponding to the D band which is associated with the disorders or defects that occur from the resonance Raman spectra of Sp2 hybridized carbon. Both the peaks can be observed in the Raman spectra for all the hybrid nanocomposite powders. However, their intensity increases with an increase in the GO content.

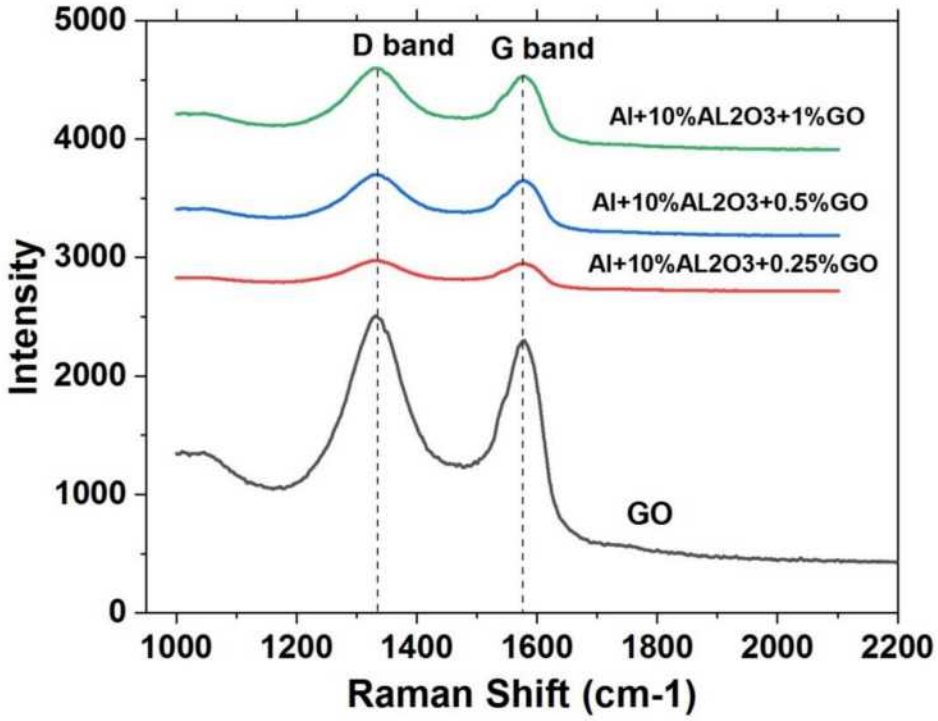

Figure 4.10 Raman spectroscopy for GO, Al-10%Al_2O_3-0.25%GO, Al-10%Al_2O_3-0.5%GO, and Al-10%Al_2O_3-1%GO hybrid nanocomposites samples

4.2.6 XRD analysis of the nanocomposite and hybrid nanocomposite samples

Fig (4.11), shows the X-ray diffraction pattern obtained for the SPS sintered samples for pure aluminum, Al-10%Al_2O_3 nanocomposites and all the developed hybrid nanocomposite samples. The XRD pattern of Al-10% Al_2O_3 nanocomposite shows slightly higher intensity peaks for both alumina and aluminum, as compared to the hybrid nanocomposite samples. This can be attributed to the effect of ball milling time where the nanocomposite was milled for 24h while the hybrid nanocomposite powders were milled for 48 hours resulting in a more homogeneous and uniform distribution of the fillers in the aluminum matrix. However, GO phase was not observed in the hybrid nanocomposite due to its very small amount. However, it was observed that no chemical reaction occurred between GO and Al- Al_2O_3 nanocomposite as there was no new phase such as

intermetallic phases or formation of aluminum carbide (Al_4C_3) was observed in any of the XRD patterns for the hybrid nanocomposites.

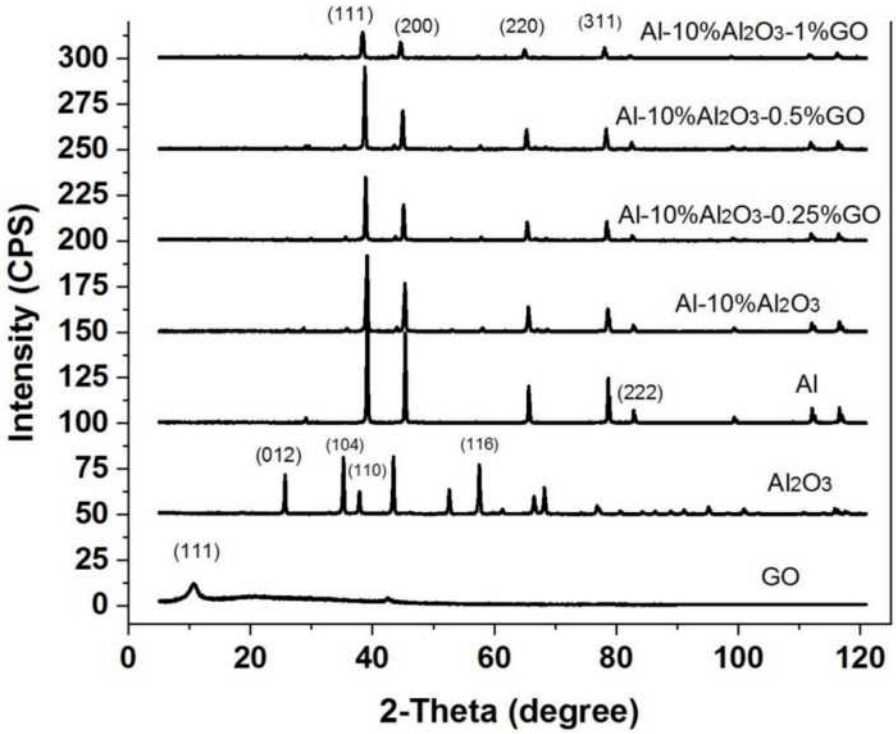

Figure 4.11 XRD for un-reinforced material(GO, Al_2O_3, Al) developed nanocomposite samples(Al-10%Al_2O_3) and hybrid nanocomposite(Al-10%Al_2O_3-0.25, 0.5, 1% GO)

4.2.7 Summary of Phase II

From the above results, it can be concluded that the hybrid nanocomposite sample containing 0.25%GO showed the highest hardness, density and uniform distribution of the fillers in the parent matrix. Hence, based upon the above results Al-10%Al_2O_3-0.25%GO was selected for further processing.

4.3 Results from Phase III

Mechanical and thermal characterizations of the optimum hybrid nanocomposite which was obtained from Phase II to be Al-10 vol% Al_2O_3-0.25 wt.% GO are evaluated. Compressive strength, differential scanning calorimetry and thermal expansions for the hybrid nanocomposite are investigated and the results are presented.

4.3.1 Evaluation of Compressive strength for Al, (Al-10%Al_2O_3) and (Al-10%Al_2O_3-0.25%GO) nanocomposites

The results of compressive strength for aluminum as reference matrix, Al-10% Al_2O_3 and the Al-10% Al_2O_3- 0.25%GO hybrid nanocomposite are presented in Fig (4.12). It can be observed that the compressive strength of aluminum sample was 75MPa which significantly increased to 130 MPa for the Al-10% Al_2O_3 nanocomposite, whereas, the compressive strain is reduced to 0.4% as compared to the aluminum sample. This effect can be attributed to the role of the hard nano particles of Al_2O_3 which also contributed towards the grain refinement of the nanocomposite leading to an increase in the hindrance to the dislocation movements. Moreover, the compressive strength is further increased in the Al-10% Al_2O_3-0.25%GO hybrid nanocomposite to a values of 180 MPa which is about 30% higher than the Al-10%Al_2O_3 nanocomposite. This improvement can be attributed to the presence of the uniformly distributed GO filler which in the hybrid nanocomposite, leading to an improvement in the interfacial adhesion between the alumina and aluminum without overlapping or agglomeration. However, an increase in the compressive strain for the hybrid composite sample was observed to a value of about 0.52% as compared to the 0.4% compressive strain for Al-10%Al_2O_3 nanocomposite. This is can be attributed to the structure of GO which contains hydroxide (OH^-) and (O^-) chains, which in turn, will lead to increase C-C bonds length at each hexagonal lattice as described in section (2.6.2)[7], these bonds will be

dominant over van der waals attractions in (Al-10%Al_2O_3-0.25%GO) hybrid nanocomposites, thus results in strain improvement caused by the efficent load trasfer from soft matrix to hard GO.[41]

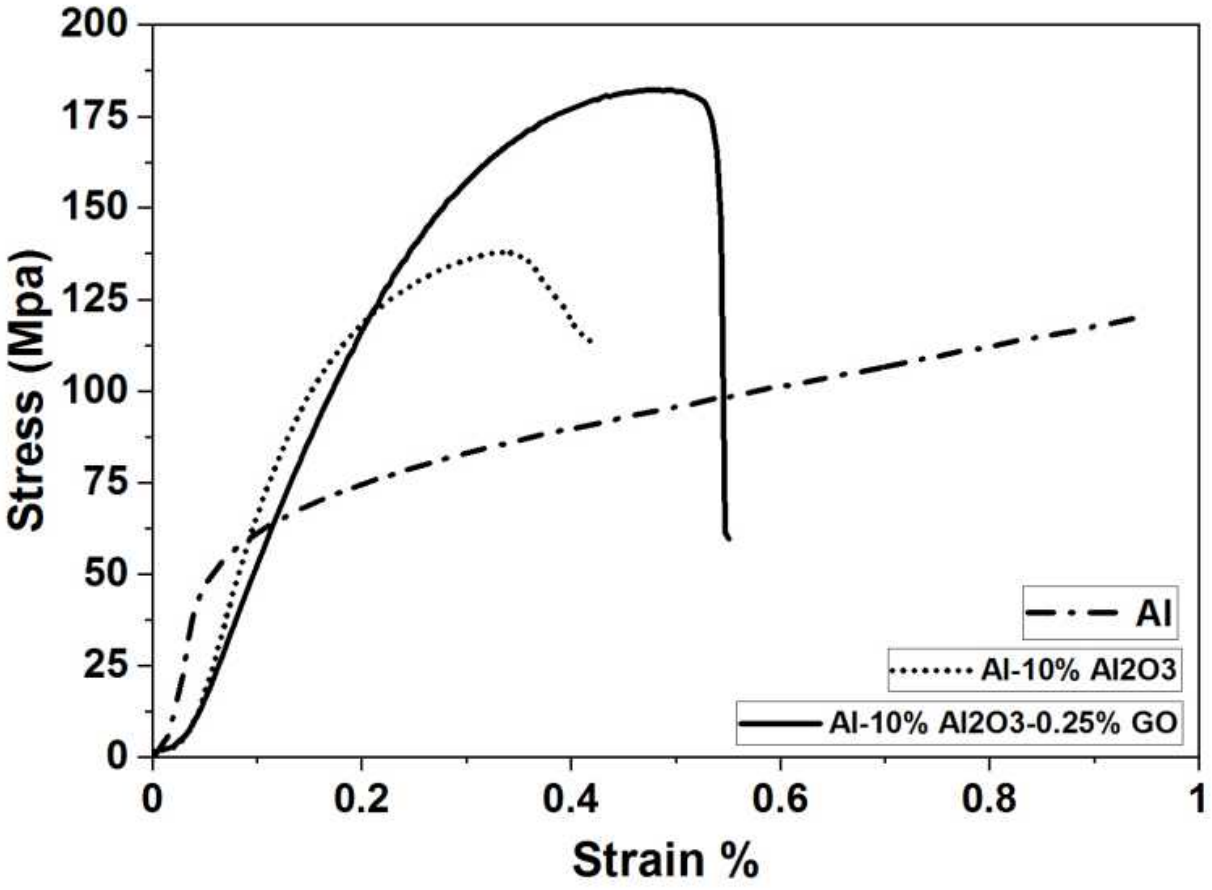

Figure 4.12 Compression test for Al, Al-10%Al_2O_3 and Al-10%Al_2O_3-0.25% GO

4.3.2 Differential scanning calorimetry (DSC) measurements for Al, (Al-10%Al_2O_3) and (Al-10%Al_2O_3-0.25%GO) nanocomposites

The DSC thermographs are shown in Fig 4.13 for pure aluminum, Al-10% Al_2O_3 and the Al-10% Al_2O_3- 0.25%GO hybrid nanocomposite. As can be observed the endothermic peak appeared at 667˚C for the pure aluminum sample. The melting point decreased on the addition of 10% Al_2O_3

to about 665 ˚C. In contrast, almost similar melting point as that of pure aluminum was observed for the hybrid composite sample to be in the range of (667-668 ˚C). However, the area under the peak decreased which constitutes the energy required to change the phase into a melting phase with the addition of 10% Al_2O_3 and a further reduction is observed on the addition of 0.25% GO. This is strongly correlated to the impurities/fillers incorporated within the matrix, whereby, Al_2O_3 contributes to the higher thermal conductivity of the composite as its thermal conductivity by a factor of 38.5- 72W/m.K [40] as compared to that of pure aluminum which approximately (205-234 W/m.K) [43]. Hence, the energy required to reach out to the melting phase is less as compared to pure aluminum sample. Likewise, GO in the hybrid nanocomposite contributes further higher to the thermal conductivity by approximately 700-2000 W/m.K based on the thickness of the layers and oxygen content of GO [42] as compared to Al-10%Al_2O_3 nanocomposite. So, the energy required to reach out to the melting phase is much lesser due to the thermal conductivity acquired by Al_2O_3 and GO. However, no major change in the melting temperature was observed. Therefore, presence of the two fillers in the hybrid nanocomposite imparts a higher thermal conductivity to the hybrid nanocomposite resulting in a reduction in the heat flow and energy required to reach out to the melting phase[44]. Data obtained from DSC is presented in Table (4.4).

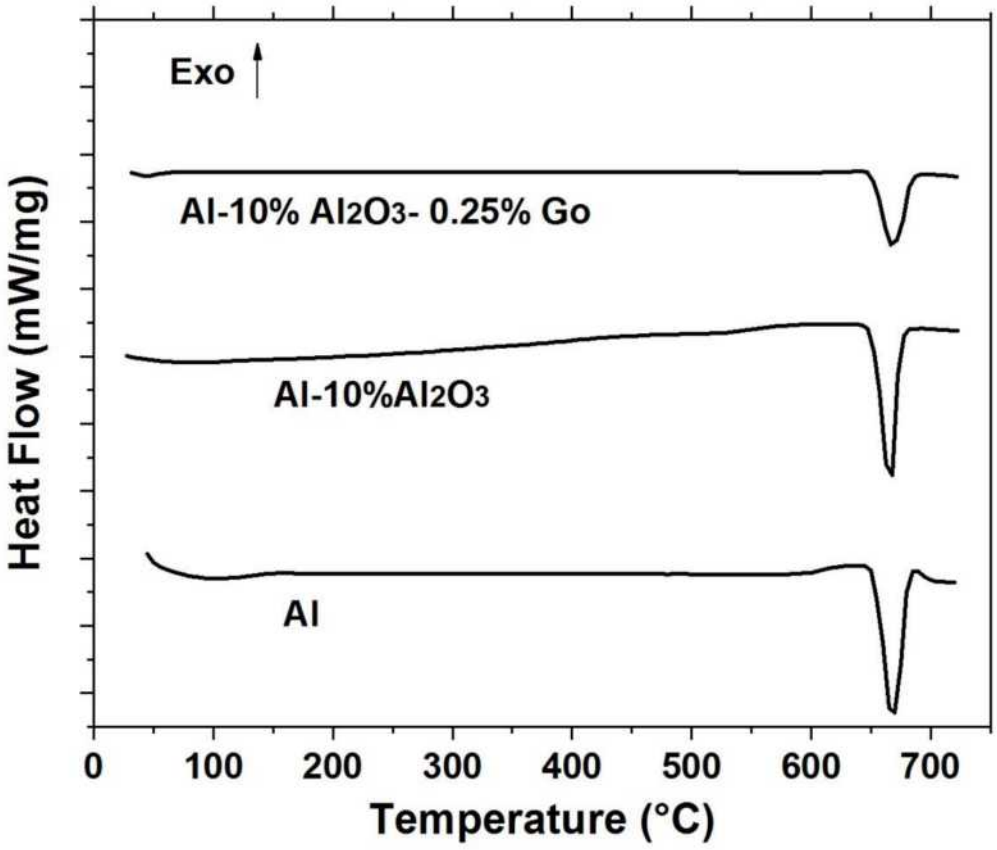

Figure 4.13 DSC for Al, Al-10%Al_2O_3 and Al-10%Al_2O_3-0.25%GO.

Table 4.4 DSC data for the developed samples Al, Al-10%Al_2O_3 and Al-10%Al_2O_3-0.25%GO.

Samples	Melting point ˚C	Heat flow (mW/mg)	Area J/g
Al	667	-4.75	-411.2
Al-10% Al_2O_3	665	-3.94	-387.2
Al-10% Al_2O_3-0.25% GO	667.8	-2.23	-338.2

4.3.3 Thermal expansion measurements for Al, (Al-10%Al_2O_3) and (Al-10%Al_2O_3-0.25%GO) nanocomposites

Thermal expansion measurements were carried out for the developed SPS samples, and the results obtained are presented in Fig. (4.14). It is observed that the coefficient of thermal expansion

linearly increased with increasing temperature for all the developed samples. Thermal expansion of pure aluminum which is the reference matrix was found to be 18.89 ppm˚C^-1. Whereas, for Al-10%Al_2O_3 nanocomposite it reduced to 15.51 ppm˚C^-l , leading to a reduction of 17% as compared to pure aluminum. Likewise, the thermal expansion further decreased for the Al-10% Al_2O_3-0.25%GO hybrid nanocomposite to a value of 14.82 ppm˚C^-1 , leading to a reduction of 4.4% in the coefficient of thermal expansion as compared to the Al-10%Al_2O_3 nanocomposite and reduction of 21% as compared to pure aluminum. This can be attributed to the effectiveness of both the fillers in improving the bonding with the matrix, whereby, these fillers prevent the gain growth of the nanocomposite. Summary of coefficient of thermal expansion (CTE) is presented in Table (4.5).

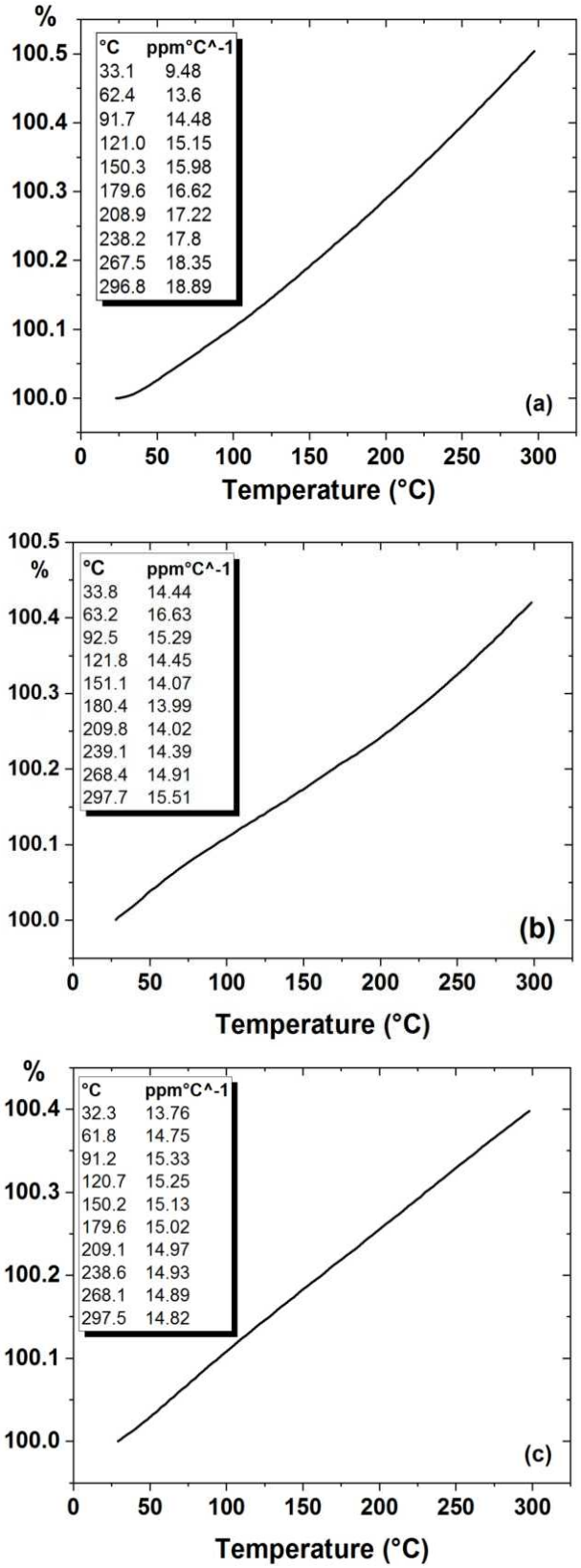

Figure 4.14. Thermal expansion of **a)** Al, **b)** Al-10%Al_2O_3, **c)** Al-10%Al_2O_3-0.25% Go

4.3.4 Summary of Phase III

From the above results, it can be concluded that the compressive strength was the highest in the hybrid nanocomposite (Al-10%Al_2O_3-0.25%GO) as a value of 180MPa compared to (Al-Al_2O_3) (130MPa) and pure aluminum (75MPa), whereas, the strain is improved in the hybrid nanocomposite from 0.4% to 0.5% as compared to (Al-10%Al_2O_3) nanocomposite. Heat flow and area associated with hybrid nanocomposite present the lowest values as compared to the aluminum and Al-10%Al_2O_3 nanocomposite samples. On the other hand, coefficient of thermal expansion was the lowest for the hybrid nanocomposite sample. As a summary, thermal and mechanical properties obtained for each sample are presented in Table (4.5). However, a comparison between this research and literature are presented in Table (4.6).

Table 4.5 Summary of mechanical and thermal properties obtained for all samples.

Test	Samples		
	Al	**Al-10%Al_2O_3**	**Al-10%Al_2O_3-0.25%GO**
Relative density (%)	99.7	97.6	96.8
Hardness (HV)	32.4	55.8	63.2
Indirect ultimate tensile strength (MPa)*	138.9	214.6	238.6
Compressive strength (MPa)	65	137	184
Thermal expansion (ppm˚C^-1)	18.89	15.51	14.82

* based on the hardness value, through the formula UTS=3.4x Brinel hardness (BH), whereby BH= (HV+10.5) /1.05

Table 4.6 Comparison between the literature and this research.

Composites	Methods	Hardness HV	Relative density %	Compressive strength (MPa)	Ultimate tensile strength (MPa)	References
Pure Al	SPS	38	99.9			[23]
Al-2vol%Al_2O_3	Ball milling and SPS	112	98			
Al-10vol%Al_2O_3		147	99.5			
Al-15vol%Al_2O_3		91	92			
Pure Al	Agate mortar and SPS	33	99.5			[25]
Al-1 vol%		37.7	98.8			
Al-5 vol%		46.9	97.1			
Al-20 vol%		56	92.5			
Al6061	Liquid stir castin	90	98.5			[45]
Al-9wt.% Al_2O_3		150	97.4			
Al-9wt.% Gr		80	98			
Al alloy 7055	Ultrasonication mixing and SPS	131.5		1000		[26]
Al-1wt% Gr		150		1200		
Al-3wt% Gr		128		750		
Al-5wt% Gr		98.6		600		
Pure Al	Cold compaction	26				[46]
Al-0.07Wt.% GO	Ultasonication and cold compaction	29				
Al-0.15Wt.% GO		30				
Al-0.3Wt.% GO		35				
Pure Al	Ball milling and tube furnace	30	98	65		[47]
Al-1wt%Go		58	90	120		
Pure Al	Ball milling and vaccum hot pressing		99.5		105	[48]
Al-0.25wt% GNS			99.13		164	
Al-0.5wt% GNS			99.08		152	
Al-1wt% GNS			99.05		138	

CHAPTER 5

CONCLUSION AND RECOMMENDATIONS

5.1 Conclusions

Hybrid aluminum nanocomposite reinforced with alumina and graphene oxide are successfully produced by powder metallurgy technique and spark plasma sintering. The study was conducted in three phases:

Phase1: Optimizing different volume percents of alumina content (10%, 20%, 30%). The following conclusions can be drawn from this phase:

- For Al- Al_2O_3 Composite, the highest hardness was obtained by adding 10 volume percent of Al_2O_3. However, on further adding alumina content, the hardness decreased.
- SEM revealed the presence of cracks along the grain boundaries in the nanocomposite sample having a higher volume percent of Al_2O_3 content.
- The highest relative density was found for the aluminum sample, while, the relative density decreased slightly in the nanocomposite samples with the addition of Al_2O_3 contents.
- Agglomeration of Al_2O_3 were found in the nanocomposite samples containing 20% and 30% of alumina content. Moreover, a non-uniform distribution of $Al_2O_3$was also observed by SEM.

- Al-10vol%Al_2O_3 exhibited the best hardness and uniform distribution of Al_2O_3 particles and hence was selected for the next phase of study.

Phase 2: Optimizing different weight percents of graphene oxide (0.25%, 0.5%, 1%) to be reinforced with the optimum volume content of alumina resulting from phase1. The following conclusions can be drawn from the results of this phase.

- The relative density decreased in the hybrid nanocomposite samples with the addition of GO content.
- Highest hardness for the hybrid nanocomposite was obtained for 0.25 wt.% of GO, while a further increase in GO content to 0.5 and 1wt%, gradually reduced the hardness.
- The microstructure of aluminum hybrid nanocomposites the presence agglomerations of GO in the hybrid nanocomposite sample containing 0.5 and 1wt% GO.
- The distribution of GO was identified to be along the grain boundaries while the alumina distributed within the grains.
- Al-10vol%Al_2O_3-0.25wt%GO hybrid nanocomposite exhibited the best properties in terms of hardness and uniform distribution of GO within the matrix and hence it was selected for further evaluation of mechanical and thermal properties in the next phase.

Phase3: Conduct the mechanical/thermal testing for the optimum hybrid nanocomposite. The following conclusions can be drawn from the above research:

- Al-10 vol%Al_2O_3-0.25 wt.% GO hybrid nanocomposite showed the least heat flow as compared to the Al-10%Al_2O_3 nanocomposite and pure aluminum.

- Al-10 vol%Al_2O_3-0.25 wt.%GO hybrid nanocomposite showed a 30% increase in the compressive strength as compared to pure aluminum.
- Al-10 vol%Al_2O_3-0.25 wt.%GO hybrid nanocomposite showed the least thermal expansion as compared to the Al-10%Al_2O_3 and pure aluminum.

5.2 Future Work

Producing Al-Al_2O_3-GO hybrid composite is promising material toward the industrial development. So, it is recommended to:

1) Study the tribological aspects of the developed hybrid nanocomposites.
2) Study the corrosion behavior for the developed hybrid nanocomposites.

REFRENCES

1- Torralba, J., Costa, C. D., & Velasco, F. (2003). P/M Aluminum matrix composites: an overview. Journal of Materials Processing Technology, 133(1-2), 203-206. doi:10.1016/s0924-0136(02)00234-0.

2- N.Chawla and K.K.Chawla (2006). "Metal Matrix Composites". New York: Springer.

3- Muley, A. V., Aravindan, S., & Singh, I. (2015). Nano and hybrid Aluminum based metal matrix composites: an overview. Manufacturing Review, 2, 15. doi:10.1051/mfreview/2015018.

4- https://www.Graphenea.com/pages/Graphene#.WWopHk_fpyJ

5- Sharma, P., Khanduja, D., & Sharma, S. (2014). Tribological and mechanical behavior of particulate Aluminum matrix composites. Journal of Reinforced Plastics and Composites, 33(23), 2192-2202. doi:10.1177/0731684414556012.

6- Berman, D., Erdemir, A., & Sumant, A. V. (2014). Graphene: a new emerging lubricant. Materials Today, 17(1), 31-42. doi:10.1016/j.mattod.2013.12.003.

7- Pop, E., Varshney, V., & Roy, A. K. (2012). Thermal properties of Graphene: Fundamentals and applications. MRS Bulletin, 37(12), 1273-1281. doi:10.1557/mrs.2012.203

8- http://www.explainthatstuff.com/Graphene.html

9- Benton, M. (1997). Introduction to composite materials. Rancho Santa Fe, CA: Mission Press.

10- Ghomashchi, M., & Vikhrov, A. (2000). Squeeze casting: an overview. Journal of Materials Processing Technology, 101(1-3), 1-9. doi:10.1016/s0924-0136(99)00291-5

11- T.W.Clyne, (2001), "Metal Matrix Composites: Matrices and Processing".

12- C. Suryanarayana (2001) "Mechanical alloying and milling", Progress in Materials Science, Vol.46, Pages 1-184.

13- Making a ball mill for fireworks book. (n.d.). Retrieved July 15, 2017, from http://fireworksnews.com/Item/M2

14- Manoj Gupta, Nai Mui Ling Sharon, "Magnesium, Magnesium Alloys, and Magnesium Composites", John Wiley and Sons, 2011.

15- Degraeuwe, J., Brauns, E., Overstraeten, R. V., Roos, J., & Govaerts, R. (1980). Sintering Mechanisms in Base Metal Conductors. ElectroComponent Science and Technology, 7(1-3), 113-118. doi:10.1155/apec.7.113.

16- V. Viswanathan, T. Laha, K. Balani, A. Agarwal, S. Seal, (2006), "Challenges and advances in nanocomposite processing techniques", Material Science and Engineering R 54, 121-285.

17- J.R. Groza, A. Zavaliangos (2003), "Nanostructured bulk solids by field activated sintering", Journal of Advanced Material Science, Volume 5,Pages 24-33.

18- N.Chawla and K.K.Chawla (2006). "Metal Matrix Composites". New York: Springer.

19- Akbari, M. K., Baharvandi, H., & Mirzaee, O. (2013). Fabrication of nano-sized Al2O3 reinforced casting Aluminum composite focusing on preparation process of reinforcement powders and evaluation of its properties. Composites Part B: Engineering, 55, 426-432. doi:10.1016/j.compositesb.2013.07.008.

20- Sajjadi, S., Ezatpour, H., & Beygi, H. (2011). Microstructure and mechanical properties of Al– Al_2O_3 micro and nano composites fabricated by stir casting. Materials Science and Engineering: A, 528(29-30), 8765-8771. doi:10.1016/j.msea.2011.08.052.

21- Özyürek, D., Tekeli, S., Güral, A., Meyveci, A., & Gürü, M. (2010). Effect of Al_2O_3 amount on microstructure and wear properties of Al–Al_2O_3 metal matrix composites prepared using mechanical alloying method. Powder Metallurgy and Metal Ceramics, 49(5-6), 289-294. doi:10.1007/s11106-010-9235-3.

22- Mazahery, A., Abdizadeh, H., & Baharvandi, H. (2009). Development of high-performance A356/nano-Al2O3 composites. Materials Science and Engineering: A, 518(1-2), 61-64. doi:10.1016/j.msea.2009.04.014.

23- Saheb, N., Khan, M. S., & Hakeem, A. S. (2015). Effect of Processing on Mechanically Alloyed and Spark Plasma Sintered Al-Al2O3Nanocomposites. Journal of Nanomaterials, 2015, 1-13. doi:10.1155/2015/609824.

24- Kang, Y., & Chan, S. L. (2004). Tensile properties of nanometric Al_2O_3 particulate-reinforced Aluminum matrix composites. Materials Chemistry and Physics, 85(2-3), 438-443. doi:10.1016/j.matchemphys.2004.02.002.

25- Dash, K., Chaira, D., & Ray, B. (2013). Synthesis and characterization of aluminium–Alumina micro- and nano-composites by spark plasma sintering. Materials Research Bulletin, 48(7), 2535-2542. doi:10.1016/j.materresbull.2013.03.014.

26- Tian, W., Li, S., Wang, B., Chen, X., Liu, J., & Yu, M. (2016). Graphene-reinforced Aluminum matrix composites prepared by spark plasma sintering. International Journal of Minerals, Metallurgy, and Materials, 23(6), 723-729. doi:10.1007/s12613-016-1286-0.

27- Bastwros, M., Kim, G., Zhu, C., Zhang, K., Wang, S., Tang, X., & Wang, X. (2014). Effect of ball milling on Graphene reinforced Al6061 composite fabricated by semi-solid sintering. Composites Part B: Engineering, 60, 111-118. doi:10.1016/j.compositesb.2013.12.043.

28- Nieto, A., Lahiri, D., & Agarwal, A. (2012). Synthesis and properties of bulk Graphene nanoplatelets consolidated by spark plasma sintering. Carbon, 50(11), 4068-4077. doi:10.1016/j.carbon.2012.04.054.

29- Wang, J., Li, Z., Fan, G., Pan, H., Chen, Z., & Zhang, D. (2012). Reinforcement with Graphene nanosheets in Aluminum matrix composites. Scripta Materialia, 66(8), 594-597. doi:10.1016/j.scriptamat.2012.01.012.

30- Pérez-Bustamante, R., Bolaños-Morales, D., Bonilla-Martínez, J., Estrada-Guel, I., & Martínez-Sánchez, R. (2014). Microstructural and hardness behavior of Graphene-nanoplatelets/Aluminum composites synthesized by mechanical alloying. Journal of Alloys and Compounds, 615. doi:10.1016/j.jallcom.2014.01.225.

31- Rashad, M., Pan, F., Tang, A., & Asif, M. (2014). Effect of Graphene Nanoplatelets addition on mechanical properties of pure Aluminum using a semi-powder method. Progress in Natural Science: Materials International, 24(2), 101-108. doi:10.1016/j.pnsc.2014.03.012.

32- Rengifo, S., Zhang, C., Harimkar, S., Boesl, B., & Agarwal, A. (2017). Tribological Behavior of Spark Plasma Sintered Aluminum-Graphene Composites at Room and Elevated Temperatures. Technologies, 5(1), 4. doi:10.3390/technologies5010004.

33- http://accuratus.com/alumox.html.

34- Bisht, A., Srivastava, M., Kumar, R. M., Lahiri, I., & Lahiri, D. (2017). Strengthening mechanism in Graphene nanoplatelets reinforced Aluminum composite fabricated through spark plasma sintering. Materials Science and Engineering: A, 695, 20-28. doi:10.1016/j.msea.2017.04.009.

35- Bodunrin, M. O., Alaneme, K. K., & Chown, L. H. (2015). Aluminium matrix hybrid composites: a review of reinforcement philosophies; mechanical, corrosion and tribological characteristics. Journal of Materials Research and Technology, 4(4), 434-445. doi:10.1016/j.jmrt.2015.05.003.

36- Suryakumari, T., Ranganathan, S., & Shankar, P. (2015). Study on Mechanical Properties of Al 7075 Hybrid Metal Matrix Composites. Applied Mechanics and Materials, 813-814, 230-234. doi:10.4028/www.scientific.net/amm.813-814.230.

37- Singh, V., Joung, D., Zhai, L., Das, S., Khondaker, S. I., & Seal, S. (2011). Graphene based materials: Past, present and future. Progress in Materials Science, 56(8), 1178-1271. doi:10.1016/j.pmatsci.2011.03.003.

38- Ravichandran, M., Vidhya, V., & Anandakrishanan, V. (2016). Study of the Characteristics of AL 5 wt.% TiO2 6 wt.% GR Hybrid P/M Composite Powders Prepared by the Process of Ball Milling. Materials Science, 51(4), 589-597. doi:10.1007/s11003-016-9880-x.

39- "Mechanical Properties of Graphene Oxide: A Molecular Dynamics Study." Taylor & Francis,

40- Alumina - Aluminium Oxide - Al_2O_3 - A Refractory Ceramic Oxide. 6 Feb. 2001,

41- Rashad, Muhammad, et al. "Investigation on Microstructural, Mechanical and Electrochemical Properties of Aluminum Composites Reinforced with Graphene Nanoplatelets." *Progress in Natural Science: Materials International*, Elsevier, 31 Oct. 2015,

42- Mahanta, Nayandeep. Thermal Conductivity of Graphene and Graphene Oxide Nano platelets - IEEE Conference Publication, 13th Intersociety Conference on Thermal and Thermomechanical Phenomena in Electronic Systems, 2012.

43- Hust, J. G., and A. B. Lankford. Thermal Conductivity of Aluminum, Copper, Iron, and Tungsten for Temperatures from 1 K to the Melting Point. National Bureau of Standards, 1984.

44- Fukuchi, Kohei, et al. "Aluminium Based High Thermal Conductive Composites Containing CNT and VGCF -Deformation Dependence of Thermal Conductivity-." *Procedia Engineering*, Elsevier, 10 June 2011,

45- Nagaral, Madeva, et al. “Mechanical Behavior of Al6061-Al2O3 and Al6061-Graphite Composites.” Materials Today: Proceedings, Elsevier, 20 Oct. 2017,

46- Liu, Jinghang, et al. “Graphene Oxide and Graphene Nanosheet Reinforced Aluminium Matrix Composites: Powder Synthesis and Prepared Composite Characteristics.” Materials & Design, Elsevier, 8 Jan. 2016,

47- Asgharzadeh, Hamed, and Maryam Sedigh. “Synthesis and Mechanical Properties of Al Matrix Composites Reinforced with Few-Layer Graphene and Graphene Oxide.” Journal of Alloys and Compounds, Elsevier, 1 Sept. 2017,

48- Li, Gang, and Bowen Xiong. “Effects of Graphene Content on Microstructures and Tensile Property of Graphene-Nanosheets / Aluminum Composites.” Journal of Alloys and Compounds, Elsevier, 13 Dec. 2016,

VITAE

Name: Tawfeeq Saad Alahmari

Date of Birth: 13, June, 1988

Place of Birth: Abha, Saudi Arabia.

Address: Al-Tahliah, Al-khubar 34716- 6638,
Saudi Arabia

Email: tawfeeqalahmari@gmail.com

Educational Qualifications:

Master of science (Mechanical Engineering)
May 2020
King Fahd University of Petroleum and Minerals
Dhahran, Saudi Arabia

Bachelor of Engineering (Mechanical)
June 2007
King Khalid University, Abha
Saudi Arabia

Industrial Experience:

Saudi Steel Pipe Company (SSP), Dammam
(Dec,2011 – April, 2014)

Vallurec Seamless Pipe Company, Dammam
(April,2014 – March,2015)

Saudi Basic Industries Corporation (SABIC), Al-Jubail
(March,2015- Present)

Achievement:

Tawfeeq Saad Alahmari, M. Abdul Samad, Tahar Laoui, Abbas Hakeem, Ihsan-Ul-Haq Toor, Faheemuddin Patel, "Mechanical and Thermal Characterization of Aluminum Hybrid Nanocomposite Reinforced with Alumina and Graphene Oxide".